1 **Impact of air pollution control measures and regional transport on**

2 **carbonaceous aerosols in fine particulate matter in urban Beijing,**

3 **China: Insights gained from long-term measurement**

4 Dongsheng Ji[1, 2*], Wenkang Gao[1, 2], Willy Maenhaut[3*], Jun He[4], Zhe Wang[1, 5], Jiwei Li[1, 6], Wupeng

5 Du[7], Lili Wang[1, 2], Yang Sun[1, 2], Jinyuan Xin[1, 2], Bo Hu[1, 2], Yuesi Wang[1, 2*]

6 *[1] State Key Laboratory of Atmospheric Boundary Layer Physics and Atmospheric Chemistry,*

7 *Institute of Atmospheric Physics, Chinese Academy of Sciences, Beijing, 100191, China*

8 *[2] Atmosphere Sub-Center of Chinese Ecosystem Research Network, Institute of Atmospheric Physics,*

9 *Chinese Academy of Sciences, Beijing, 100191, China*

10 *[3] Department of Chemistry, Ghent University, Gent, 9000, Belgium*

11 *[4] Natural Resources and Environment Research Group, International Doctoral Innovation Centre,*

12 *Department of Chemical and Environmental Engineering, University of Nottingham Ningbo China,*

13 *Ningbo, 315100, China*

14 *[5] Research Institute for Applied Mechanics, Kyushu University, Fukuoka, 816-8580, Japan*

15 *[6] University of Chinese Academy of Sciences, Beijing, 100049, China*

16 *[7] Institute of Urban Meteorology, Chinese Academy of Meteorological Sciences, Beijing, 100081,*

17 *China*

19 Correspondence to: Dongsheng Ji (jds@mail.iap.ac.cn), Willy Maenhaut (Willy.Maenhaut@UGent.be)

20 and Yuesi Wang (wys@dq.cern.ac.cn)

Abstract As major chemical components of airborne fine particulate matter ($PM_{2.5}$), organic carbon (OC) and elemental carbon (EC) have vital impacts on air quality, climate change, and human health. Because OC and EC are closely associated with fuel combustion, it is helpful for the scientific community and policymakers assessing the efficacy of air pollution control measures to study on the impact of the control measures and regional transport on the OC and EC levels. In this study, hourly mass concentrations of OC and EC associated with $PM_{2.5}$ were semi-continuously measured from March 2013 to February 2018. The results showed that annual mean OC and EC concentrations declined from 14.0 to 7.7 $\mu g/m^3$ and from 4.0 to 2.6 $\mu g/m^3$, respectively, from March 2013 to February 2018. In combination with the data of OC and EC in previous studies, an obvious decreasing trend in OC and EC concentrations was found, which was caused by clean energy policies and effective air pollution control measures. However, no obvious change in the ratios of OC and EC to the $PM_{2.5}$ mass (on average, 0.164 and 0.049, respectively) was recorded, suggesting that inorganic ions still contributed a lot to $PM_{2.5}$. Based on the seasonal variations of OC and EC, it appeared that higher OC and EC concentrations were still observed in the winter months, with the exception of winter of 2017-2018. Traffic policies executed in Beijing resulted in nighttime peaks of OC and EC, caused by heavy-duty vehicles and heavy-duty diesel vehicles being permitted to operate from 0:00 to 6:00. In addition, the fact that there was no traffic restriction in weekends led to higher concentrations in weekends compared to weekdays. Significant correlations between OC and EC were observed throughout the study period, suggesting that OC and EC originated from common emission sources, such as exhaust of vehicles and fuel combustion. OC and EC levels increased with enhanced SO_2, CO and NO_x concentrations while the O_3 and OC levels enhanced simultaneously when O_3 concentrations were higher than 50 $\mu g/m^3$. Nonparametric wind regression analysis was performed to examine the sources of OC and EC in the Beijing area. It was found that there were distinct hot spots in the northeast wind sector at wind speeds of approximately 5 km/h, as well as diffuse signals in the southwestern wind sectors. Source areas further away from Beijing were assessed by potential source contribution function (PSCF) analysis. A high-potential source area was precisely pinpointed, which was located in the northwestern and southern areas of Beijing in 2017 instead of solely in the southern areas of Beijing in 2013. This work shows that improvement of the air quality in Beijing benefits from strict control measures; however, joint prevention and

51 control of regional air pollution in the regions is needed for further improving the air quality. The

52 results provide a reference for controlling air pollution caused by rapid economic development in

53 developing countries.

54

55 **Key words** air pollution control measures, regional transport, organic carbon, elemental carbon,
56 Beijing

57

1 Introduction

Worldwide attention on atmospheric organic carbon (OC) and elemental carbon (EC) has been paid by the public and the scientific community because OC and EC have vital effects on air quality, atmospheric visibility, climate, and human health (Bond et al., 2013; Boucher et al., 2013; World Health Organization (WHO), 2012). OC is composed of thousands of organic compounds and occupies 10-50 % of the ambient $PM_{2.5}$ mass (Seinfeld and Pandis, 1998) while EC, which is emitted from fuel combustion, represents 1-13 % of the ambient $PM_{2.5}$ mass (Shah et al., 1986; Tao et al., 2017; Malm et al., 1994). Considering that OC and EC occupy high fractions of the $PM_{2.5}$, a decline in OC and EC concentrations will improve air quality. Due to the light scattering potential of OC and the light absorption ability of EC, high concentrations of OC and EC can impair the atmospheric visibility. In addition, OC and EC can affect the atmospheric energy balance through scattering and absorbing incoming and outgoing solar and terrestrial radiation (direct effect) and through modifying the microphysical properties of clouds, like influencing cloud condensation nuclei and/or ice nuclei (indirect effects). Direct and indirect effects of OC and EC remain one of the principal uncertainties in estimates of anthropogenic radiative forcing (Boucher et al., 2013). In particular, black carbon (BC also called EC) coated with secondary particles can enhance aerosol radiative forcing (Wang et al., 2013; Zhang et al., 2008). BC is found to aggravate haze pollution in megacities (Ding et al., 2016; Zhang et al., 2018). Most of all, OC and EC adversely affect human health. As important constituents of OC, polycyclic aromatic hydrocarbons (PAHs) are well known as carcinogens, mutagens, and teratogens and therefore pose a serious threat to the health and the well-being of humans (Boström et al., 2002). Short-term epidemiological studies provide sufficient evidence of all-cause and cardiovascular mortality and cardiopulmonary hospital admissions associated with daily variations in BC concentrations; besides, cohort studies proved that all-cause and cardiopulmonary mortality are linked with long-term average BC exposure (WHO, 2012). Thus, long-term continuous observations of OC and EC are a prerequisite to further study air quality, atmospheric visibility, climate effects, and human health. However, long-term continuous observations of OC and EC in China are scarce.

In the world, China is considered as one of the regions of high emissions of OC and EC due to high energy consumption and increasing vehicle population, accompanying rapid economic

87   development and urbanization for decades (http://www.stats.gov.cn/tjsj/ndsj/2017/indexch.htm). As

88   the capital of China, Beijing with a residential population of 21.7 million, domestic tourists of

89   2.9×10^2 million and foreign tourists of approximately 3.3 million in 2017

90   (http://tjj.beijing.gov.cn/English/AD/) faces severe air pollution problems, which have attracted

91   worldwide attention. A series of studies on OC and EC have already been performed in Beijing.

92   Lang et al. (2017) indicated that OC showed a downward trend and EC had almost no change before

93   2003, both increased from 2003 to 2007, but decreased after 2007. The decline in OC concentrations

94   was associated with coal combustion and motor vehicle emission control measures, while that in

95   EC was caused by the replacement of fossil fuel and control of biomass emissions. Tao et al. (2017)

96   stated that the nearly 30 % reduction in total carbon (TC) in recent years in Beijing can be taken as

97   a real trend. Lv et al. (2016) found that the concentrations of OC and EC remained unchanged from

98   2000 to 2010 in Beijing. Yang et al. (2011a) conducted a long-term study of carbonaceous aerosol

99   from 2005 to 2008 in urban Beijing and found a decline in the ratio of carbonaceous species to the

100    $PM_{2.5}$ mass in contrast to what was observed 10 years earlier, which indicated that the importance

101   of carbonaceous species in $PM_{2.5}$ had decreased. In addition, pronounced seasonal variations were

102   recorded with the highest concentrations occurring in winter and the lowest ones in summer. Overall,

103   these previous researches seem somewhat inconsistent with each other and they seldom focused on

104   studying the impact of air pollution control measures and regional transport on the carbonaceous

105   aerosol levels in detail.

106   Notably, a series of the strictest measures on emission abatement and pollution control were

107   implemented in China from September 2013 (Jin et al., 2016). Substantial manpower and material

108   resources have been put into improving the air quality in the past five years and significant measures

109   are being taken for the atmospheric environment and ecosystem (Gao et al., 2017). To evaluate the

110   effectiveness of air pollution control measures, it is necessary to conduct a long-term continuous

111   observation of OC and EC and to study their long-term variation. Most of the previous studies

112   showed average information for certain periods based on filter sampling and laboratory analysis and

113   did not reflect the dynamic evolution processes of OC and EC with hourly resolution, which can

114   provide important and detailed information for the potential health risk in the area with frequent

115   occurrence of air pollution episodes. In addition, long-term measurements in urban areas of China

116 with high population density were scarce (Yang et al., 2005, 2011a; Zhang et al., 2011; Li et al.,

117 2015; Chang et al., 2017) and the knowledge on long-term continuous hourly observations is still

118 lacking, which is yet important for recognizing the influence of source emissions on air quality.

119 Based on the-above mentioned background, it is necessary to perform a long-term continuous

120 hourly observation to explore the characteristics of OC and EC, to examine the relationship between

121 OC and EC and with major air pollutants and their sources so as to better assess the influence of

122 emission control measures on the OC and EC levels. In this study, inter-annual, seasonal, weekly

123 and diurnal variation of OC and EC were investigated. The influence of local and regional

124 anthropogenic sources was evaluated using non-parametric wind regression (NWR) and potential

125 contribution source function (PSCF) methods. This study will be helpful for improving the

126 understanding of the variation and sources of OC and EC associated with $PM_{2.5}$ and assessing the

127 effectiveness of local and national PM control measures and it provides a valuable dataset for

128 atmospheric modelling study and assessing the health risk. It also is the first time that a continuous

129 hourly measurement for a 5-year period based on the thermal-optical method is reported for urban

130 Beijing.

131 **2 Experimental**

132 **2.1 Description of the site**

133 The study site (39°58'28'' N, 116°22'16'' E, 44 m above ground) was set up in the second floor

134 in the campus of the State key laboratory of atmospheric boundary physics and atmospheric

135 chemistry of the Institute of atmospheric Physics, Chinese Academy of Science (Fig. 1). The site is

136 approximately 1 km south from the 3rd Ring Road (main road), 1.2 km north from the 4th Ring

137 Road (main road), 200 m west of the G6 Highway (which runs north-south) and 50 m south of the

138 Beitucheng West Road (which runs east-west), respectively. The annual average vehicular speeds in

139 the morning and evening traffic peaks were approximately 27.8 and 24.6 km/h, respectively, in the

140 past five years. During the whole study period the level of traffic congestion is mild based on the

141 traffic performance index published by the Beijing Traffic Management Bureau

142 (http://www.bjtrc.org.cn/), which indicated 1.5-1.8 times more time will be taken to publicly travel

143 during traffic peaks than during smooth traffic. The study site is surrounded by residential zones, a

144 street park and a building of ancient relics without industrial sources. The experimental campaign

was performed from March 1, 2013 to February 28, 2018. The periods of March 1, 2013 to February 28, 2014, March 1, 2014 to February 28, 2015, March 1, 2015 to February 28, 2016, March 1, 2016 to February 28, 2017 and March 1, 2017 to February 28, 2018 are, hereinafter, called for short 2013, 2014, 2015, 2016 and 2017, respectively.

2.2 Instrumentation

Concentrations of $PM_{2.5}$-associated OC and EC were hourly measured with semi-continuous thermal-optical transmittance method OC/EC analyzers (Model 4, Sunset Laboratory Inc. Oregon, Unite states of America (USA)). The operation and maintenance are strictly executed according to standard operating procedures (SOP, https://www3.epa.gov/ttnamti1/spesunset.html). Volatile organic gases are removed by an inline parallel carbon denuder installed upstream of the analyzer. A round 16-mm quartz filter is used to collect $PM_{2.5}$ with a sampling flow rate of 8 L/m. A modified NIOSH thermal protocol (RT-Quartz) is used to measure OC and EC. The sampling period is 30 min and the analysis process lasts for 15 min. Calibration is performed according to the SOP. An internal standard CH_4 mixture (5.0 %; ultra-high purity He) is automatically injected to calibrate the analyzer at the end of every analysis. In addition, off-line calibration was conducted with an external amount of sucrose standard (1.06 μg) every three months. The quartz fiber filters used for sample collection were replaced by new ones before the laser correction factor dropped below 0.90. After replacement, a blank measurement of the quartz fiber filters is carried out. The uncertainty of the TC measurement has been estimated to be approximately ±20 % (Peltier et al., 2007). The analyzers/monitors for O_3, CO, SO_2, NO_x and $PM_{2.5}$, and their precision, detection limits and calibration methods have been described in detail elsewhere (Ji et al., 2014). Briefly, O_3 was measured using an ultraviolet photometric analyzer (model 49i, Thermo Fisher Scientific (Thermo), USA), CO with a gas filter correlation nondispersive infrared method analyzer (model 48i, Thermo, USA), SO_2 using a pulsed-fluorescence analyzer (model 43i, Thermo, USA), $NO-NO_2-NO_x$ with a chemiluminescence analyzer (model 42, Thermo, USA) and $PM_{2.5}$ using a US Environmental Protection Agency Federal Equivalent Method analyzer of $PM_{2.5}$ (SHARP 5030, Thermo, USA). Meteorological data such as wind speed (WS), wind direction (WD), relative humidity (RH) and atmospheric temperature (T) were recorded via an automatic meteorological station (Model AWS310; Vaisala, Finland). The data were processed using an Igor-based software (Wu et al., 2018)

174   and the commercial software of Origin.

175   **2.3 NWR and PSCF methods**

176   **2.3.1 NWR method**

177   NWR is a source-to-receptor source identification model, which provides a meaningful

178   allocation of local sources (Henry et al., 2009; Petit et al., 2017). Wind analysis results using NWR

179   were obtained using a new Igor-based tool, named ZeFir, which can perform a comprehensive

180   investigation of the geographical origins of the air pollutants (Petit et al., 2017). The principle of

181   NWR is to smooth the data over a fine grid so that concentrations of air pollutants of interest can be

182   estimated by any couple of wind direction (θ) and wind speed (u). The smoothing is based on a

183   weighing average where the weighing coefficients are determined using a weighting function $K(\theta,$

184    $u, \sigma, h) = K_1 (\theta, \sigma) \times K_2 (u, h)$ (i.e., Kernel functions). The estimated value (E) given θ and u is

185   calculated by the following equations (1)-(3):

186    $$E(\theta|u) = \frac{\sum_{i=1}^{N} K1\left(\frac{\theta - Wi}{\sigma}\right) \times K2\left(\frac{u - Yi}{h}\right) \times Ci}{\sum_{i=1}^{N} K1\left(\frac{\theta - Wi}{\sigma}\right) \times K2\left(\frac{u - Yi}{h}\right)} \qquad (1)$$

187    $$K_1(x) = \frac{1}{\sqrt{2\pi}} \times e^{-0.5x^2} \qquad -\infty < x < \infty \qquad (2)$$

188    $$K_2(x) = 0.75 \times (1 - x^2) \qquad -1 < x < 1 \qquad (3)$$

189   where σ and h were smoothing parameters, which can be suggested by clicking on the button of

190   suggest estimate in the software of Zefir; Ci, Wi, and Yi are the observed concentration of a pollutant

191   of interest, resultant wind speed and direction, respectively, for the ith observation in a time period

192   starting at time t_i; N is the total number of observations.

193   After the calculation, graphs of the estimated concentration and the joint probability are

194   generated. The NWR graph of the air pollutant of interest, acquired directly via the NWR calculation,

195   represents an integrated picture of the relationship of estimated concentration of the specific

196   pollutant, wind direction and wind speed. The graph of the joint probability for the wind data,

197   equivalent to a wind rose, shows the occurrence probability distribution of the wind speed and wind

198   direction.

199   **2.3.2 PSCF method**

200   The PSCF method is based on the residence time probability analysis of air pollutants of

201   interest (Ashbaugh et al., 1985). Source locations and preferred transport pathways can be identified

(Poirot and Wishinski, 1986; Polissar et al., 2001; Lupu and Maenhaut, 2002). The potential locations of the emission sources are determined using backward trajectories. A detailed description can be found in Wang et al. (2009). In principle, the PSCF is expressed using equation (4):

$$PSCF(i, j) = w_{ij} \times (m_{ij}/n_{ij}) \tag{4}$$

where w_{ij} is an empirical weight function proposed to reduce the uncertainty of n_{ij} during the study period, m_{ij} is the total number of endpoints in (i, j) with concentration value at the receptor site exceeding a specified threshold value (the 75th percentiles for OC and EC each year were used as threshold values to calculate m_{ij}) and n_{ij} is the number of back-trajectory segment endpoints that fall into the grid cell (i, j) over the period of study. The National Oceanic and Atmospheric Administration Hybrid Single-Particle Lagrangian Integrated Trajectory model (https://ready.arl.noaa.gov/HYSPLIT.php) was used for calculating the 48-h backward trajectories terminating at the study site at a height of 100 m every 1 h from March 1 2013 to February 28 2018. In this study, the domain for the PSCF was set in the range of (30-70 °N, 65-150 °E) with the grid cell size of 0.25 × 0.25°.

3 Results and discussion

3.1 Levels of OC and EC

Statistics for the OC and EC concentrations from March 1, 2013 to February 28, 2018 are summarized in Table 1. Benefiting from the Air Pollution Prevention and Control Action Plan and increasing atmospheric self-purification capacity (ASC, shown in Table S1), a decline in annual average concentrations is on the whole recorded. In detail, the annual average concentrations of both OC and EC peaked in 2014 and then started to decline gradually during the remainder of the study period. Nonetheless, the annual average concentrations of $PM_{2.5}$ were generally decreasing from 2013 to 2017. To assess whether the decreases are statistically significant, 2-tailed paired t-tests were applied for OC, EC and $PM_{2.5}$ using their monthly average concentrations in 2013 and 2016 as paired datasets. At a confidence level of 98%, from March to October, the paired data are statistically different, indicating that the concentrations of OC, EC and $PM_{2.5}$ declined during the above period from 2013 to 2016; however, the concentrations of OC, EC and $PM_{2.5}$ during November and February from 2013 to 2016 are not statistically different. The decline in OC and EC concentrations is closely associated with decreasing coal consumption, increasing usage of natural

231   gases and the implementation of a stricter vehicular emission standard and increasing atmospheric

232   self-purification capacity (Tables S1-S3). Knowledge of the relative contribution of OC and EC to

233    $PM_{2.5}$ is important in formulating effective control measures for ambient PM (Wang et al., 2016a).

234   The ratios of OC and EC to $PM_{2.5}$ varied little during the whole study period, suggesting that

235   vehicular emission might be an important contributor of OC and EC although several other pollution

236   sources also contributed to the OC and EC loadings. The ratios of OC to $PM_{2.5}$ ranged from 15.5 to

237   17.8 % with the average of 16.4 %, while those of EC to $PM_{2.5}$ ranged from 4.5 to 5.2 % with the

238   average of 4.9 %. OC accounted, on average, for 77.0 ± 9.3 % of the total carbon (TC, the sum of

239   OC and EC), while EC amounted for 23.0 ± 9.3 % of the TC. These results are consistent with those

240   in previous studies (Wang et al., 2016a; Tao et al., 2017, Lang et al., 2017). The contribution of TC

241   to $PM_{2.5}$, 21.3 ± 15.8 %, is also similar to those reported in previous studies, listed in Table S4, for

242   example, at urban sites of Hongkong, China (23.5-23.6 % in 2013), Hasselt (23 %) and Mechelen

243   (24 %) in northern Belgium, rural sites in Europe (19-20 %) and some sites in India (on average,

244   20 %, Bisht et al., 2015; Ram and Sarin, 2010; Ram and Sarin, 2012), but lower than those observed

245   historically at multiple sites in China (on average 27 %, Wang et al., 2016a), with Beijing (27.6 %,

246   from March 2005 to Feb 2006), Chongqing (28.3 %, from March 2005 to February 2006), Shanghai

247   (34.5 %, from March 1999 to May 2000) and Guangzhou (26.4 %, December 2008 to February

248   2009), in Budapest (40 %), Istanbul (30 %), and many sites in the USA, like Fresno (43.2 %), Los

249   Angeles (36.9 %) and Philadelphia (33.3 %) (Na et al., 2004). Compared to previous studies in

250   Beijing (Table S4), the TC to $PM_{2.5}$ ratio became smaller in this study, indicating a relatively lower

251   contribution from carbonaceous aerosols to $PM_{2.5}$ in this study. The difference in the TC/$PM_{2.5}$ ratio

252   could be ascribed to two factors. One factor is the difference in characteristics of sampling locations

253   between that in our study and those in the earlier studies. However, our site and those in the previous

254   studies used for comparison are all located in urban areas of Beijing (Chaoyang and Haidian district,

255   respectively). It is reasonable to assume that they are affected by common sources since the

256   surrounding environments exhibit similar features. Besides, the annual average $PM_{2.5}$

257   concentrations in both districts published by the Ministry of Environmental Protection, China

258   (http://106.37.208.233:20035/) were quite comparable to each other from 2013 to 2017 ($y=0.99x$,

259    $r^2=0.92$), indicating that both areas had particle pollution of a similar degree. The other factor is that

the contribution from secondary inorganic ions to the $PM_{2.5}$ became more important because of a stronger atmospheric oxidation capacity (the annual average O_3 concentrations were 102, 109, 116, 119, and 136 $\mu g/m^3$, respectively, from 2013 to 2017 in the Beijing-Tianjin-Hebei region; published by http://106.37.208.233:20035/), which could give rise to a lower TC to $PM_{2.5}$ ratio. A higher TC to $PM_{2.5}$ ratio suggests that there is a lower contribution from secondary inorganic ions to $PM_{2.5}$, while a lower ratio may indicate a larger contribution from secondary inorganic ions to $PM_{2.5}$. The carbonaceous aerosol (the sum of multiplying the measured OC by a factor of 1.4 and EC) represented on average, 27.7 ± 16.7 % of the observed $PM_{2.5}$ concentration, making it a dominant contributor to $PM_{2.5}$.

Table 3 lists recently published results for OC and EC mass concentrations in major megacities. Although the observation periods were not same, a comparative analysis of OC and EC concentrations between different megacities could show the status of energy consumption for policymakers, drawing lessons and experience from other countries. It is obvious that the $PM_{2.5}$-associated OC and EC levels in the megacities in the developing countries were far higher than those in the developed countries. The $PM_{2.5}$-associated OC and EC concentrations in Beijing were higher than those in Athens, Greece (2.1 and 0.54 $\mu g/m^3$), Los Angeles (2.88 and 0.56 $\mu g/m^3$) and New York (2.88 and 0.63 $\mu g/m^3$), USA, Paris, France (3.0 and 1.4 $\mu g/m^3$), Soul, South Korea (4.1 and 1.6 $\mu g/m^3$), Tokyo, Japan (2.2 and 0.6 $\mu g/m^3$) and Toronto, Canada (3.39 and 0.5 $\mu g/m^3$). That is because clean energy has widely been used and strict control measures are taken to improve the air quality step by step in the developed countries. Of the megacities in the developing countries, OC and EC concentrations in Beijing were lower than those in most other megacities, like Mumbai and New Delhi, India, and Xi'an and Tianjin, China, but close to those in Shanghai and Hongkong, China, and higher than those in Lhasa, China. These differences/similarities indicate that OC and EC gradually declined in Beijing and that a series of measures had progressive effects. However, to further improve the air quality, more synergetic air pollution abatement measures of carbonaceous aerosols and volatile organic compounds (VOCs) emissions need to be performed.

Fig. 2 shows the mass fractions of carbonaceous aerosols in different $PM_{2.5}$ levels classified according to $PM_{2.5}$ concentrations during the whole study period. There were 571, 561, 310, 169, 142 and 74 days for excellent, good, slightly polluted, moderately polluted, heavily polluted and

severely polluted air quality levels during the whole period. It was obvious that OC and EC concentrations increased with the degradation of air quality. OC and EC concentrations were 6.3 and 1.7, 10.2 and 2.9, 13.7 and 4.1, 17.3 and 5.3, 24.6 and 7.9 and 35.5 and 11.3 $\mu g/m^3$ for excellent, good, slightly polluted (LP), moderately polluted (MP), heavily polluted (HP) and severely polluted (SP) air quality days, respectively. However, the percentages of OC and EC accounting to $PM_{2.5}$ decreased with the deterioration of air quality. OC and EC made up for 31.5 % and 8.3 %, 18.9 % and 5.4 %, 14.7 % and 4.4 %, 13.4 % and 4.1 %, 12.9 % and 4.2 % and 11.4 % and 3.6 % during excellent, good, slightly polluted, moderately polluted, heavily polluted and severely polluted air quality days, respectively. The percentage for OC decrease from 31.4 to 11.4 % while that for EC decreased from 8.3 to 3.6 % with the deterioration of air quality, indicating that other $PM_{2.5}$ constituents than OC and EC contributed more to the increased $PM_{2.5}$ levels. This is consistent with previous studies showing that secondary inorganic ions play a more important role in the increase in $PM_{2.5}$ concentrations (Ji et al., 2014, 2018).

3.2 Inter-annual variation of OC and EC

To evaluate the effect of the clean air act over a prolonged period, our OC and EC data were combined with the data of previous studies for Beijing (He et al., 2011; Zhao et al., 2013; Ji et al., 2016; Tao et al., 2017; Lang et al., 2017). As shown in Fig. 3, a decreasing trend in OC and EC concentrations is on the whole observed. Table S2 summarizes a variety of policies and actions to reduce pollutant emissions in power plants, coal-fired boilers, residential heating and traffic areas in Beijing since 2002. Although the gross domestic product, population, energy consumption and vehicular population rapidly increased (Table S3), the general decreasing trends in OC and EC concentrations could be attributed to the combined effect of the more stringent traffic emission standards and traffic restriction, the energy structure evolving from intensive coal and diesel consumption to replacement with natural gas and electricity, and retrofitting with SO_2 and NO_2 removal facilities to meet the new emission standards applicable to different coal-fired facilities, etc. In particular, there is an obvious dividing line of OC and EC concentrations in 2010. After 2010, the OC and EC concentrations became substantially lower than those observed previously. In addition to the measures mentioned in Table S2, the relocation of Shougang Corporation, which is one of the China's largest steel companies, and other highly polluting factories out of Beijing might have

helped to some extent; all the small coal mines in Beijing were shut down and plenty of yellow label (heavy-polluting) vehicles were forced off road. Note that the OC and EC levels in 2008 and 2009 were also somewhat lower, which was caused by a series of radical measures to improve the air quality for the Olympic Games in 2008 and a decline in industrial production because of China's exports crash in 2009, respectively. It suggests that a stringent clean air act and rectifying industry played important roles in the air quality improvement.

In this study, the fire spots were counted in the domain of (30-70° N, 65-150° E) using the MODIS Fire Information for Resource Management System (Giglio, 2013). Note also that the effective control of biomass burning might contribute to the decrease in OC and EC concentrations. In Fig. 3, it can be seen that the annual average EC concentration and fire spot counts exhibit a rather similar variation from 2004 to 2017, except in the year 2012, which suggests that the EC levels are somewhat correlated with the biomass burning; this might indicate that biomass burning contributed somewhat to the EC levels. The reduction in fire spot counts from 2014 to 2017, which resulted from efforts to control the agricultural field residue burning since 2013, helped to reduce the EC concentrations to some extent, but the low EC levels during 2014-2017 are likely mostly due to the implementation of the clean air act. With regard to the anomaly in the year 2012, based on the MODIS data for this year, a very non-uniform distribution of fire spots in the BTH region was observed, with a distinct decrease of fire spot counts in Beijing, but higher fire spot counts in the southern Hebei Province; this may be ascribed to the fact that the policy of Banning Straw Burning in Summer and Autumn was executed to different degrees in the whole region, with better implementation in Beijing area and worse action in the other parts. (http://www.beijing.gov.cn/zfxxgk/110029/qtwj22/2012-12/11/content_357114.shtml). In addition, for the years from 2002 to 2017, the highest precipitation volume in Beijing was recorded in 2012, i.e., 733.2 mm, and the rainy days mainly occurred in the intensive straw burning periods, accounting for 76.4% of all rainy days in 2012. The frequent wet scavenging might have suppressed the EC concentrations during the intensive straw burning periods, so that the annual EC level for 2012 was comparable to those recorded from 2011 onward.

Similar to OC and EC, the annual mean SO_2 and NO_2 concentrations also showed a decreasing trend. As well-known, SO_2 originates from coal combustion and sulfur-containing oil (Seinfeld and

Pandis, 1998). With the replacement of coal for industrial facilities, residential heating and cooking by clean energy (e.g., natural gases, electricity and lower sulfur content in oil), a clear decline in annual SO_2 concentrations was observed in the Beijing area starting from 2002. As compared to SO_2, the annual decreasing rate of NO_2 was relatively lower. Besides the power plants and other boilers, traffic emissions are another major source of NO_2. The rapid increase of vehicle population may partly offset the great effort in reducing coal consumption to lower the NO_2 level despite the transition to more stringent traffic emission standards.

3.3 Monthly and seasonal variations

Fig. S1 shows the monthly mean OC and EC concentrations at our study site for the whole 5-year period. Similar variations are observed with generally higher mean OC and EC levels in the cold season (from November to March next year when the centralized urban residential heating is provided) and lower ones in the warm season (from April to October). The highest average OC and EC concentrations were 24.1 ± 18.7 μg/m^3 in December 2016 and 9.3 ± 8.5 μg/m^3 in December 2015, respectively. However, the lowest OC and EC levels were not observed in the warm months; they were 5.0 ± 4.6 μg/m^3 in January, 2018 and 1.5 ± 1.7 μg/m^3 in December, 2017, respectively; this was associated with both frequent occurrence of cold air mass and the implementation of a winter radical pollution control action plan (Chen and Chen, 2019) in Beijing from November, 2017. Overall, the increased fuel consumption for domestic heating in addition to unfavorable meteorological conditions (lower mixing layer height, temperature inversion and calm wind) in the colder months is considered to lead to higher OC and EC levels (Ji et al., 2014). In addition, the lower air temperature in the cold months led to shifting the gas-particle equilibrium of semi-volatile organic compounds (SVOCs) into the particle phase, leading to the higher OC levels. In the cold months, the cold start of vehicles (5.64 million vehicles in Beijing at the end of 2017) also increased the emission of OC. In the warm season, lower OC and EC levels were observed, which could be attributed to the following factors: no extra energy consumed for domestic heating, strong wet scavenging by frequent precipitation occurring in these months, and more unstable atmospheric conditions favorable for pollutant dispersion; in addition, during this period, the monthly mean OC and EC concentrations generally decreased from year to year. In contrast, for the cold season, the monthly mean OC and EC concentrations did not show a clear decreasing trend from year to year

376 except for October. In addition to the more intensive energy consumption in the cold season, the EC

377 and OC levels could also be enhanced strongly by regional transport and stagnant meteorology

378 leading to ground surface accumulation in the autumn and winter (Wang et al., 2019; Yi et al., 2019);

379 this would have counteracted the efficacy of the energy structure change in the Beijing-Tianjin-

380 Hebei region in the past few years. It is worth pointing out that, on a year to year basis, the monthly

381 average OC and EC concentrations in the cold seasons of 2017 and 2018 were generally lower than

382 those in 2016, demonstrating to some extent the effectiveness of the execution of the radical

383 pollution control measures for cities on the air pollution in the Beijing-Tianjin-Hebei region. The

384 interquartile ranges of OC and EC in the warm months were narrower than in the cold months,

385 indicating that there was more substantial variation in concentration in the latter months. The larger

386 variation in the colder months could be caused by the cyclic accumulation and scavenging processes.

387 In this region, due to these processes, the concentration of particulate matter increases rapidly when

388 the air mass back trajectories change from the northwest and north to the southwest and south over

389 successive days in Beijing; in contrast, the concentration of particulate matter declines sharply when

390 a cold front causes a shift of back trajectories from the southwest and south to the north and

391 northwest (Ji et al., 2012). The accumulation processes are closely associated with unfavorable

392 meteorological conditions, which give rise to higher OC and EC concentrations, while more

393 scavenging of aerosols by cold fronts leads to lower levels.

394   As to the seasonality in OC and EC, similar seasonal variations are observed in the various

395 years with generally higher mean concentrations in autumn and winter and lower levels in spring

396 and summer (Fig. 4). Remarkably, the OC and EC concentrations in the autumn and winter of 2017

397 were lower than those in the previous years. This was due to the combined effect of controlling

398 anthropogenic emissions strictly and favorable meteorological conditions. Since September 2017, a

399 series of the most stringent measures within the Action Plan on Prevention and Control of Air

400 Pollution was implemented to improve the air quality; these measures included restricting industrial

401 production by shutting down thousands of polluting plants, suspending the work of iron and steel

402 plants in 28 major cities and limiting the use of vehicles and reducing coal consumption as a heating

403 source in northern China. In addition, the air quality improvement in the autumn and winter of 2017

404 was closely tied to frequent cold fronts accompanied by strong winds, which was favorable for

dispersing the pollutants. The average OC and EC concentrations in the winter were 1.69 and 1.14, 2.17 and 1.93, 1.49 and 2.14, 2.41 and 2.29 and 0.80 and 0.88 times higher than those in the summer for 2013, 2014, 2015, 2016 and 2017, respectively. The difference in the ratios for 2017 was due to the series of the most stringent measures taking effect and favorable meteorology. The Beijing municipal government in particular has made great efforts to replace coal by natural gases and electricity-powered facilities. Besides, new energy vehicles are increasingly used to replace the gasoline vehicles.

3.4 Diurnal variation and weekly pattern for OC and EC

As can be seen in Figs. S2 and S3, a clear diurnal variation is observed for both OC and EC in each year. This variation is closely tied to the combined effect of diurnal variation in emission strength and evolution of the PBL. The pattern for EC with higher concentrations in the nighttime (from 20:00 to 4:00) and lower levels in the daytime (from 9:00 to 16:00) is largely linked to the vehicular emissions. The EC concentrations increased starting from 17:00, corresponding with the evening rush hours, emission from nighttime heavy-duty diesel trucks (HDDT) and heavy-duty vehicles (HDV) and the formation of a nocturnal stable PBL. As regulated by the Beijing Traffic management Bureau (http://www.bjjtgl.gov.cn/zhuanti/10weihao/), HDV and HDDT are allowed to enter the urban area inside the 5th Ring Road from 0:00 to 06:00 (local Time). At other times, both the higher PBL height and lower traffic intensity resulted in lower EC concentrations. The amplitude of the diurnal variation in the EC concentrations was smaller in the last three years. The maximum peak concentration (22:00-7:00) was 1.68, 1.62, 1.43, 1.40 and 1.40 times higher than that observed in the valley period (13:00-15:00) for 2013, 2014, 2015, 2016 and 2017, respectively. Similar to EC, the diurnal pattern for OC was also characterized by higher concentrations in the nighttime (from 20:00 to 4:00) and lower levels in the daytime (from 14:00 to 16:00). However, the formation of secondary organic carbon from gas-phase oxidation of VOCs with increased solar radiation during midday gave rise to a small additional peak of OC. Like for EC, the amplitude of the diurnal variation in the OC concentrations was smaller in the last three years. The maximum peak concentration (19:00-3:00) was 1.47, 1.47, 1.30, 1.34 and 1.26 times higher than that observed in the valley period (14:00-16:00) for 2013, 2014, 2015, 2016 and 2017, respectively. It was pity that no diurnal variation in traffic counts can be available but the hourly average traffic counts in 2015,

434 2016 and 2017 could be found in (Beijing Transportation Annual Report,

435 http://www.bjtrc.org.cn/JGJS.aspx?id=5.2&Menu=GZCG). Considering that the hourly average

436 traffic counts varied little in urban Beijing and they were 5969/hr, 5934/hr and 6049/hr in 2015,

437 2016 and 2017, respectively, the small amplitude of the diurnal variation in the last three years might

438 be related to local emission intensities; these might have been significantly affected by the

439 enforcement of a series of traffic emission control measures since 2015, including more strict

440 restriction of emission from heavy-duty diesel vehicle public buses, wider usage of electric public

441 buses, and scrappage of all the high-emitting (yellow-labelled) vehicles, etc. (Tab. S2). All these

442 actions led to a decline in emissions of OC and EC and narrowed the amplitude of the diurnal

443 variation in the EC concentration.

444 Separate diurnal variations of OC and EC for each season in each year are shown in Figs S4

445 and S5. Similar patterns are observed in in the four seasons but the difference between peak and

446 valley levels is larger in the winter than in the other three seasons. The larger variation in the winter

447 is due to the additional emission from residential heating and more unfavorable meteorological

448 conditions (Ji et al., 2016).

449 The difference in diurnal pattern between weekdays and weekends was also examined, see Figs.

450 S6 and S7. Similar diurnal variations are found on weekdays and weekend days. The maximum

451 peak concentration for EC (22:00-7:00) was 1.55, 1.43, 1.55, 1.51, 1.51, 1.46 and 1.59 times higher

452 than the valley concentration (13:00-15:00) for Monday, Tuesday, Wednesday, Thursday, Friday,

453 Saturday and Sunday, respectively, while the maximum peak concentration for OC (19:00-3:00)

454 was 1.41, 1.32, 1.38, 1.43, 1.37, 1.31 and 1.43 times higher than the valley concentration (14:00-

455 16:00) for Monday, Tuesday, Wednesday, Thursday, Friday, Saturday and Sunday, respectively. In

456 contrast to previous studies (Grivas et al., 2012; Jeong et al., 2017; Chang et al., 2017), OC and EC

457 exhibited statistically significant higher concentrations on weekends than on weekdays in this study

458 (statistically significant based on the analysis of the weekly data using t-test statistics, $p<0.05$). The

459 average OC and EC concentrations on Saturday and Sunday were 13.2 ± 11.8 μg/m^3 and 3.9 ± 2.7

460 μg/m^3 and 12.0 ± 10.4 μg/m^3 and 3.7 ± 3.6 μg/m^3, respectively, whereas the average OC and EC

461 levels during the weekdays were 11.8 ± 10.8 μg/m^3 and 3.6 ± 3.5 μg/m^3, respectively. This indicates

462 that there is no significant decline in anthropogenic activity in the weekends compared to weekdays.

In fact, enhanced anthropogenic emissions could be caused by no limit on driving vehicles based on license plate on weekends. The larger OC and EC concentrations in the weekend are thus mainly attributed to enhanced traffic emissions, which is consistent with higher NO_2 and CO concentrations in the weekend (on average 56.6 ± 35.9 μg/m^3 for NO_2 and 1.16 ± 1.18 mg/m^3 for CO on weekdays (number of samples = 29492); 57.8 ± 37.0 μg/m^3 for NO_2 and 1.25 ± 1.18 mg/m^3 for CO on weekends (number of samples = 11881)).

3.5 Relationship between OC and EC and with gaseous pollutants

The relationship between particulate OC and EC is an important indicator that can give information on the origin and chemical transformation of carbonaceous aerosols (Chow et al., 1996). Primary OC and EC are mainly derived from vehicular emissions, coal combustion, biomass burning, etc. in urban areas (Bond, et al., 2013). Primary OC and EC could correlate well with each other under the same meteorology. However, the correlation would become gradually less significant with the enhancement of secondary OC formation via complex chemical conversion of VOCs (gas-to-particle or heterogeneous conversion). In addition, it should be noted that EC is more stable than OC (Bond, et al., 2013). Hence, the relationship between OC and EC can to some extent be used as a parameter reflecting the source types and contributions (Blando and Turpin, 2000). Fig. 5 presents the regression between the OC and EC concentrations for the PM$_{2.5}$ samples of the separate years 2013 to 2017. Significant correlations (R^2 ranging from 0.87 to 0.66) were observed with the slopes declining from 3.6 to 2.9 throughout the study period. The significant correlations suggest that in most cases OC and EC originated from similar primary sources. The slopes are consistent with the OC/EC ratios ranging from 2.0 to 4.0 for urban Beijing in previous studies (He et al., 2001; Dan et al., 2004; Zhao et al., 2013; Ji et al., 2016). In addition, the average OC/EC ratios observed in this study are comparable to those observed at other urban sites with vehicular emission as a dominant source in China and foreign countries, but lower than those in cities where coal is an important source of the energy needed (Table 3). The decline in the OC/EC ratio may be caused by decline in coal consumption and restriction in biomass burning. Coal combustion, biomass burning and secondary formation give rise to higher OC/EC ratios while vehicular emission result in lower ones (Cao et al., 2005).

491   EC and part of the OC originate from primary anthropogenic emissions, including fossil fuel

492   combustion and biomass burning (Bond et al., 2013), and secondary OC is formed along with ozone

493   formation. Hence, long-term and concurrent measurement of OC, EC, SO_2, NO_x, CO and O_3 is

494   helpful for understanding the emission features or formation processes and for providing tests to

495   current emission inventories. The variation in the OC and EC as a function of the SO_2, NO_x, CO

496   and O_3 concentration is shown in Fig. 6. There is a clear increase in OC and EC with increasing

497   SO_2, NO_x and CO, suggesting that the latter played a role in the enhancement of the former and that

498   these various species shared common sources although they have a different lifetime. OC and EC

499   increased, on average, by approximately 8.9 $\mu g/m^3$ and 5.7 $\mu g/m^3$, respectively, with an increase of

500   2 mg/m^3 in CO. Considering that CO has a long lifetime (Liang et al., 2004) and that its increase

501   depends on source strength and meteorology, high CO concentrations usually occur in the heating

502   season when unfavorable meteorological conditions prevail. At very high CO concentrations, the

503   increase in OC becomes slower than that in EC. This can be explained by that local emissions

504   became dominant because the unfavorable meteorological conditions corresponding with the high

505   CO concentrations resulted in a weak exchange of air on the regional scale. The OC/EC ratio

506   declined at very high CO concentrations. This could be because vehicular emissions played an

507   important role in the OC and EC loadings (Ji et al., 2019). As documented by previous studies

508   (Schauer et al., 2002, Na et al., 2004), emission of gasoline vehicles results in an OC/EC ratio

509   varying from 3 to 5 while that of diesel vehicles is below 1. The above results are consistent with

510   previous studies which showed that gasoline and diesel vehicles give rise to higher CO emissions

511   (Wu et al., 2016).

512   Given that NO_x and CO have some common emission sources (Hassler et al., 2016), the OC

513   and EC levels were also analyzed in different intervals of NO_x concentrations. Both OC and EC are

514   enhanced with increasing NO_x concentrations. Their enhancements were 5.0 $\mu g/m^3$ and 2.1 $\mu g/m^3$,

515   respectively, for an increase in NO_x concentration of 40 $\mu g/m^3$. Although NO_x are highly reactive

516   and have a short lifetime (Seinfeld and Pandis, 1998) in contrast to CO, the OC/EC ratio also

517   declined at very high NO_x concentrations, be it to a lesser extent than was the case at very high CO

518   concentrations. As was the case for high CO concentrations, more stable meteorological conditions

519   and local emissions became prevailed when higher concentrations of NO_x were observed. In fact,

520   63.5 % of all NO_x emissions come from vehicular emissions based on the statistical data of air

521   pollutant   emissions   in   Beijing

522   (http://www.bjepb.gov.cn/bjhrb/xxgk/ywdt/zlkz/hjtj37/827051/index.html).

523   Examining the variation of OC and EC for different intervals of SO_2 concentrations allows us

524   to further study the impacts of industrial production or coal combustion on the OC and EC levels.

525   Similar to the relationship between CO and the carbonaceous species, the OC and EC concentrations

526   enhanced with increasing SO_2 concentrations. Their enhancements were 2.8 μg/m^3 and 0.7 μg/m^3,

527   respectively, for an increase in SO_2 concentration of 10 μg/m^3. An increase in the OC/EC ratio

528   occurred at large SO_2 concentrations, suggesting that coal consumption provided a substantial

529   contribution to the OC and EC levels in Beijing. Because oil with a low sulfur content has been

530   widely used in Beijing since 2008 and little coal was used in the urban areas of Beijing, the SO_2

531   mostly originated from industrial production in the surrounding areas of Beijing and from coal

532   combustion for residential heating in the suburban and rural areas of Beijing. Previous studies also

533   showed that a higher OC/EC ratio is due to coal consumption and not from vehicular emissions

534   (Cao et al., 2005). Hence, coal combustion (for industrial production) on the regional scale led to

535   the enhancement of both the OC/EC ratio and SO_2 concentrations in Beijing via long-range transport.

536   Emissions of primary air pollutants lead through multiple pathways to the formation of ozone

537   and secondary organic carbon (SOC) (Seinfeld and Pandis, 1998), both of which are the principal

538   components of photochemical smog. The relationship between OC and O_3 is of use for

539   understanding their variation and formation. The OC concentrations were highest for an O_3

540   concentration of 50 μg/m^3, which is approximately the average O_3 concentration in Beijing in winter

541   (Cheng et al., 2018). During the period of an O_3 concentration of 50 μg/m^3, low atmospheric

542   temperature (9.4±9.9 ºC), relatively high RH (59.2±23.7 %), lower WS (1.1±0.8 m/s) and higher

543   NO_x concentrations (72.7±57.5 ppb) were observed and a lower mixed layer height was recorded in

544   winter (Tang et al., 2016), which were favorable for accumulation and formation of OC. A relatively

545   lower temperature is beneficial for condensation/absorption of SVOCs into existing particles (Ji et

546   al., 2019), which would then experience further chemical reactions to generate secondary organic

547   aerosol (SOA). Note that a low temperature does not significantly reduce SOA formation rates

548   (Huang et al., 2014) in the winter. In addition, processes including aqueous-phase oxidation and

549 NO$_3$-radical-initiated nocturnal chemistry may contribute to or even dominate SOA formation

550 during winter (Hallquist et al., 2009; Rollins et al., 2012; Huang et al., 2014). Hence, the above

551 factors gave rise to the higher OC concentration at an O$_3$ concentration of 50 μg/m^3 particularly in

552 winter. In addition, scattering and absorbing effects of aerosols that were trapped in the lower mixed

553 layer height led to less solar radiation reaching the ground and further restrained the O$_3$ formation

554 in the cold season (Xing et al., 2017; Wang et al., 2016b). OC declined when O$_3$ concentrations

555 increased from 50 to 100 μg/m^3. Usually moderate O$_3$ concentrations accompanying lower OC

556 concentrations are caused by increasing T (19.5±8.3 ºC), increasing WS (2.0±1.3 m/s) and less

557 titration of relatively lower observed NO concentrations (6.4±14.6 ppb). It can also be seen that

558 there was a concurrent increasing trend of OC and ozone when the O$_3$ concentration was above 100

559 μg/m^3, which generally occurred in the warmer season. Besides the impact of meteorological

560 conditions, such a trend might not be dominated by gas-to-particle partitioning of low-volatility

561 organic compounds but by the oxidation of VOCs driven by hydroxyl radicals to generate both SOC

562 and O$_3$ with relatively long lifetimes (>12 h; Wood et al., 2010).

563 **3.6 Impact of atmospheric transport on the OC and EC concentrations**

564   Figs. 7 and 8 show the results of the NWR analysis applied to 1-h PM$_{2.5}$-associated OC and

565 EC concentrations measured from 2013 and 2017 in Beijing. Fig. S8 presents the gridded emissions

566 of OC and BC for the Beijing-Tianjin-Hebei (BTH) region and China, based on emission inventory

567 (Zheng et al., 2018). The NWR results exhibit distinct hot spots (higher concentrations) in the

568 northeast wind sector at wind speeds of approximately 0-6 km/h, which were closely associated

569 with local emissions under stagnant meteorological conditions (low wind speed), as well as diffuse

570 signals in the southwestern wind sector. The joint probability data in Figs. 7 and 8 show prevailing

571 winds were from N to E and from S to W with wind speeds of approximately 1-6 km/h and of

572 approximately 4-9 km/h, respectively. Note further that the hot spots of OC are broader than those

573 of EC in the graphs of estimated concentrations; this might be due to the fact that the VOCs (the

574 precursors of SOC) emitted from upwind areas at the relatively higher WS in contrast to EC,

575 including the SW wind sector, led to an increase in OC concentrations at the receptor site while the

576 EC concentrations slowly declined due to dilution and deposition.

577   Considering that the NWR analysis can only provide an allocation of local sources, the PSCF

analysis is a helpful complement to investigate potential advection of pollution over larger geographical scales (Petit et al., 2017). Fig. 9 presents the PSCF results for OC and EC for the years 2013 to 2017. Similar to the NWR analysis, the PSCF results indicated that local emissions and regional transport from southerly areas were important contributors to the OC and EC loadings during the whole study period. Only slight differences in the potential source regions are observed between the different years. In 2013, a clear high potential source area was recorded for both OC and EC; it was located in the southern plain areas of Beijing, particularly in the adjacent areas of the Hebei, Henan, Shandong, Anhui and Jiangsu provinces. This was because there were intensified anthropogenic emissions from those in 2013. The high pollutant emissions were caused by rapid economic growth, urbanization and increase in vehicle population, energy consumption and industrial activity in the southern plain areas of Beijing (Zhu et al., 2018), which resulted in a high aerosol loading in the downwind areas. This result is consistent with previous studies (Ren et al., 2004; Wu et al., 2014; Ji et al., 2018). In contrast to 2013, in the years 2014 to 2017 the high potential source regions for OC and EC stretched to the juncture of Inner Mongolia and the Shaanxi and Shanxi provinces, and even to the juncture of Inner Mongolia and the Ningxia Hui Autonomous Region and of Inner Mongolia and the Gansu province. This is consistent with coal power plants being abundant in the above areas (Liu F. et al., 2015). As well known, coal power plants are also important emitters of SO_2, and those emissions were seen in satellite images (Li et al., 2017; Zhang et al., 2017), thus proving evidence for those sources. The potential source areas for OC and EC were similar in 2013 and 2014. Overall, the potential source areas were more intense for OC than for EC. The emission of OC precursors (i.e., volatile organic compounds) from the Hebei, Henan, Shandong, Anhui, Jiangsu, Shanxi and Shaanxi provinces led to OC concentrations downwind via chemical conversion during the atmospheric transport. The widest potential source areas for OC and EC were recorded in 2016 and they expanded into the eastern areas of Xinjiang Uyghur Autonomous Region. They are probably associated with the economic boom in the western areas of China. In 2015, the potential source areas were like in 2013 and 2014 also more intense for OC than for EC. Although the winter action plan was enforced in Beijing, Tianjin and 26 surrounding cities (the so-called "2+26 cities"), whereby the industrial output was curtailed, inspections of polluting factories were ramped up and small-scale coal burning was banned at the end of 2017, there was still a clear

607   spatial difference in emission of air pollutants, with relatively higher $PM_{2.5}$ concentrations in the

608   southern areas of Beijing. Hence, these areas still contributed substantially to OC and EC loading

609   in Beijing.

610   As found in earlier studies (Ji et al., 2018; Zhu et al., 2018), the southern areas of Beijing were

611   main source areas. Despite the ever-stringent air pollution control measures, which are enforced in

612   key areas of China, the economic booming in the western areas of China gave rise to substantial air

613   pollution in the adjacent areas of several provinces and the northwestern areas of China. To further

614   improve the air quality in Beijing, strict emission restrictions should be launched in the above areas

615   and joint control and prevention of air pollution should be enforced on the regional scale. It should

616   be avoided that polluted enterprises, which are closed in key regions, are moved to the western areas

617   of China or to areas where there is no supervision and control of the emission of air pollutants.

618   **4 Conclusions**

619   In this study, hourly mass concentrations of OC and EC in $PM_{2.5}$ were semi-continuously

620   measured from March 1, 2013 to February 28, 2018 at a study site in Beijing. The inter-annual,

621   monthly, seasonal and diurnal variations in OC and EC are presented, the relationship between the

622   carbonaceous species and other pollutants was examined and the source regions were assessed using

623   both NWR and PSCF analysis. The impact of the air pollution control measures and of the regional

624   transport on carbonaceous species in the fine particulate matter was investigated. The following

625   main conclusions can be drawn:

626   (1) OC and EC occupied a high fraction of the observed $PM_{2.5}$ concentrations, making it a dominant

627   contributor of $PM_{2.5}$. Their concentrations increased with the degrading air quality whereas their

628   percentage in $PM_{2.5}$ declined, which was consistent with previous studies showing that secondary

629   inorganic ions played a relatively more important role in increasing $PM_{2.5}$ concentrations.

630   (2) A clear decline in OC and EC levels was observed after a series of energy policies for air

631   pollution abatement and control had been implemented. To further improve air quality, more

632   synergistic air pollution abatement measures of carbonaceous aerosols and VOCs emissions are

633   needed.

634   (3) OC and EC showed marked seasonal, monthly, weekly and diurnal variations. The seasonal

635   patterns were characterized by higher concentrations in the colder months (from November to

February) and lower ones in the warm months (from May to October) of the various years. Because of stringent measures for air pollution abatement, the difference between the winter and summer levels decreased. The EC diurnal pattern was characterized by higher concentrations in the nighttime (from 20:00 to 4:00) and lower ones in the daytime (from 9:00 to 16:00). The higher OC and EC levels during the weekend can be attributed to the traffic regulation in Beijing. The diurnal fluctuation in OC and EC was closely tied to a combined effect of change in emission sources and evolution of the PBL.

(4) Significant correlations between OC and EC were observed throughout the study period, suggesting that OC and EC originated from common sources, such as vehicle exhaust, coal combustion, etc. The contribution of coal combustion and biomass burning decreased and this resulted in lower OC/EC ratios. The OC and EC concentrations increased with higher SO_2, CO and NO_x levels, while the O_3 and OC concentrations increased simultaneously for O_3 levels above 50 $\mu g/m^3$.

(5) Local emissions and regional transport played an important role in the OC and EC concentrations. Higher concentrations were observed for winds from the northeast sector at wind speeds of approximately 5 km/h, but there were also diffuse signals in the southwestern wind sectors. The potential source regions of OC and EC stretched to the broader areas in northwestern and western regions where coal and coal power plants are abundant. Some slight differences in the potential source regions were observed from 2013 to 2017, which was closely associated with the economic boom in the western areas of China. In addition, the southern areas of Beijing still contributed a lot to OC and EC loading in Beijing.

In summary, this study will be helpful for improving the understanding the sources of OC and EC associated with $PM_{2.5}$ and for assessing the effectiveness of local and national PM control measures. In addition, it provides valuable datasets for modelling studies and for assessing the health risk.

Acknowledgements

This work was supported by the National Key Research and Development Program of China (2017YFC0210000), the Beijing Municipal Science and Technology Projects (D17110900150000 and Z171100000617002), the CAS Key Technology Talent Program, and the National research

program for key issues in air pollution control (DQGG0101 and DQGG0102). The authors would like to thank all members of the LAPC/CERN in IAP, CAS, for maintaining the instruments used in the current study. We also like to thank NOAA for providing the HYSPLIT and TrajStat model.

Author contributions

D.S., W.M. and Y.S. designed the research. D.S., W.M., J.H., Z.W., W. K., W.P., Y.S., J.Y., B.H. and Y.S. performed the research. D.S., Z.W., and W.M. analyzed the data. D.S., J.H., and W.M. wrote and edited the manuscript. All other authors commented on the manuscript.

References

Ashbaugh, L. L., Malm, W. C., and Sadeh, W. Z.: A residence time probability analysis of sulfur concentrations at Grand Canyon National Park, Atmos. Environ., 19, 1263-1270, 1985.

Bisht, D. S., Srivastava, A. K., Pipal, A. S., Srivastava, M. K., Pandey, A. K., Tiwari, S., and Pandithurai, G.: Aerosol characteristics at a rural station in southern peninsular India during CAIPEEX-IGOC: physical and chemical properties, Environ. Sci. Pollut. Res., 22, 5293-5304, 10.1007/s11356-014-3836-1, 2015.

Blando, J. and Turpin, B.: Secondary organic aerosol formation in cloud and fog droplets: a literature evaluation of plausibility, Atmos. Environ., 34 (10), 1623–1632, 2000.

Bond, T. C., Doherty, S. J. Fahey, D. W., Forster, P. M., Berntsen, T., DeAngelo, B. J., Flanner, M. G., Ghan, S., Kärcher, B., Koch, D., Kinne, S., Kondo, Y., Quinn, P. K., Sarofim, M. C., Schultz, M. G., Schulz, M., Venkataraman, C., Zhang, H., Zhang, S., Bellouin, N., Guttikunda, S. K., Hopke, P. K., Jacobson, M. Z., Kaiser, J. W., Klimont, Z., Lohmann, U., Schwarz, J. P., Shindell, D., Storelvmo, T., Warren, S. G., and Zender, C. S.: Bounding the role of black carbon in the climate system: A scientific assessment, J. Geophys. Res-Atmos., 118(11), 5380–5552, 2013.

Boström, C. E., Gerde, P., Hanberg, A., Jernström, B., Johansson, C., Kyrklund, T., Rannug, A., Torngvist, M., Victorin, K., and Westerholm, R.: Cancer risk assessment, indicators, and guidelines for polycyclic aromatic hydrocarbons in the ambient air, Environ. Health Perspect., 110, 451-488, 2002.

Boucher, O., Randall, D., Artaxo, P., Bretherton, C., Feingold, G., Forster, P., Kerminen, V. M., Kondo, Y., Liao, H., Lohmann, U., Rasch, P., Satheesh, S. K., Sherwood, S., Stevens, B., Zhang, X. Y.: Contribution of working group | to the fifth assessment report of the Intergovernmental Panel on

694 Climate Change. Clouds and aerosols. In: Stocker, T. F., Qin, D., Plattner, G. K., Tignor, M., Allen,

695 S. K., Doschung, J., Nauels, A., Xia, Y., Bex, V., Midgley, P. M., Eds. Climate change 2013: the

696 physical science basis. Cambridge University Press, Cambridge, United Kingdom and New York,

697 616–617, 2013.

698 Bressi, M., Sciare, J., Ghersi, V., Bonnaire, N., Nicolas, J. B., Petit, J. E., Moukhtar, S., Rosso, A.,

699 and Féron, A.: A one-year comprehensive chemical characterisation of fine aerosol ($PM_{2.5}$) at urban,

700 suburban and rural background sites in the region of Paris (France), Atmos. Chem. Phys., 13(15),

701 7825-7844, 2013.

702 Cao, J. J., Lee, S. C., Zhang, X. Y., Chow, J. C., An, Z. S., Ho, K. F., Watson, J. G., Fung, K., Wang,

703 Y. Q., and Shen, Z. X.: Characterization of airborne carbonate over a site near Asian dust source

704 regions during spring 2002 and its climatic and environmental significance, J. Geophys. Res.:

705 Atmos., 110, doi:10.1029/2004JD005244, 2005.

706 Chang, Y., Deng, C., Cao, F., Cao, C., Zou, Z., Liu, S., Lee, X., Li, J., Zhang, G., and Zhang, Y.:

707 Assessment of carbonaceous aerosols in Shanghai, China – Part 1: long-term evolution, seasonal

708 variations, and meteorological effects, Atmos. Chem. Phys., 17, 9945-9964,

709 https://doi.org/10.5194/acp-17-9945-2017, 2017.

710 Chen, D., Cui, H., Zhao, Y., Yin, L., Lu, Y., and Wang, Q.: A two-year study of carbonaceous

711 aerosols in ambient $PM_{2.5}$ at a regional background site for western Yangtze River Delta, China,

712 Atmos. Res., 183, 351-361, 2017.

713 Chen, H. and Chen, W.: Potential impact of shifting coal to gas and electricity for building sectors

714 in 28 major northern cities of China. Appl. Energ., 236, 1049-1061, 2019.

715 Chen, X. C., Ward, T. J., Cao, J. J., Lee, S. C., Chow, J. C., Lau, G. N. C., Yim, S. H. L., and Ho, K.

716 F.: Determinants of personal exposure to fine particulate matter ($PM_{2.5}$) in adult subjects in Hong

717 Kong, Sci. Total Environ., 628-629, 1165-1177, https://doi.org/10.1016/j.scitotenv.2018.02.049,

718 2018.

719 Chen, Y., Xie, S., Luo, B., and Zhai, C.: Characteristics and origins of carbonaceous aerosol in the

720 Sichuan Basin, China, Atmos. Environ., 94, 215-223, 2014.

721 Chen, Y., Xie, S. D., Luo, B., and Zhai, C. Z.: Particulate pollution in urban Chongqing of southwest

722 China: Historical trends of variation, chemical characteristics and source apportionment, Sci. Total

Environ., 584, 523-534, 2017

Cheng, N., Chen, Z., Sun, F., Sun, R., Dong, X., Xie, X., and Xu, C.: Ground ozone concentrations over Beijing from 2004 to 2015: Variation patterns, indicative precursors and effects of emission reduction, Environ. Pollut., 237, 262-274, https://doi.org/10.1016/j.envpol.2018.02.051, 2018.

Chow, J. C., Watson, J. G., Lu, Z., Lowenthal, D. H., Frazier, C. A., Solomon, P. A., Thuillier, R. H., and Magliano, K.: Descriptive analysis of $PM_{2.5}$ and PM_{10} at regionally representative locations during SJVAQS/AUSPEX, Atmos. Environ., 30, 2079-2112, https://doi.org/10.1016/1352-2310(95)00402-5, 1996.

Dai, Q. L., Bi, X. H., Liu, B. S., Li, L. W., Ding, J., Song, W. B., Bi, S. Y., Schulze, B. C., Song, C. B., Wu, J. H., Zhang, Y. F., Feng, Y. C., and Hopke, P. K.: Chemical nature of $PM_{2.5}$ and PM_{10} in Xi'an, China: Insights into primary emissions and secondary particle formation, Environ. Pollut. 240, 155-166, 2018.

Dan, M., Zhuang, G., Li, X., Tao, H., and Zhuang, Y.: The characteristics of carbonaceous species and their sources in $PM_{2.5}$ in Beijing, Atmos. Environ., 38, 3443-3452, https://doi.org/10.1016/j.atmosenv.2004.02.052, 2004.

Ding, A. J., Huang, X., Nie, W., Sun, J. N., Kerminen, V. M., Petäjä, T., Su, H., Cheng, Y. F., Yang, X. Q., Wang, M. H., Chi, X. G., Wang, J. P., Virkkula, A., Guo, W. D., Yuan, J., Wang, S. Y., Zhang, R. J., Wu, Y. F., Song, Y., Zhu, T., Zilitinkevich, S., Kulmala, M., and Fu, C. B.: Enhanced haze pollution by black carbon in megacities in China, Geophys. Res. Lett., 43, 2873–2879, 2016.

Duan, F., He, K., Ma, Y., Yang, F., Yu, X., Cadle, S., Chan, T., and Mulawa, P.: Concentration and chemical characteristics of $PM_{2.5}$ in Beijing, China: 2001–2002, Sci. Total Environ., 355, 264-275, 2006.

Gao, J., Woodward, A., Vardoulakis, S., Kovats, S., Wilkinson, P., Li, L., Xu, L., Li, J., Yang, J., Li, J., Cao, L., Liu, X., Wu, H., and Liu, Q.: Haze, public health and mitigation measures in China: A review of the current evidence for further policy response, Sci. Total Environ., 578, 148-157, https://doi.org/10.1016/j.scitotenv.2016.10.231, 2017.

Giglio, L.: MODIS Collection 5 Active Fire Product User's Guide Version 2.5 http://earthdata.nasa.gov/files/MODIS_Fire_Users_Guide_2.5.pdf, 2013.

Grivas, G., Cheristanidis, S., and Chaloulakou, A.: Elemental and organic carbon in the urban

752 environment of Athens. Seasonal and diurnal variations and estimates of secondary organic carbon,

753 Sci. Total Environ., 414, 535-545, 2012.

754 Hallquist, M., Wenger, J., Baltensperger, U., Rudich, Y., Simpson, D., Claeys, M., Dommen, J.,

755 Donahue, N. M., George, C., Goldstein, A. H., Hamilton, J. F., Herrmann, H., Hoffmann, T., Iinuma,

756 Y., Jang, M., Jenkin, M. E., Jimenez, J. L., Kiendler-Scharr, A., Maenhaut, W., McFiggans, G.,

757 Mentel, Th. F., Monod, A., Prevot, A. S. H., Seinfeld, J. H., Surratt, J. D., Szmigielski, R., and Wildt,

758 J.: The formation, properties and impact of secondary organic aerosol: current and emerging issues,

759 Atmospheric Chemistry and Physics 9(14), 5155-5236, 2009.

760 Hassler, B., McDonald, B. C., Frost, G. J., Borbon, A., Carslaw, D. C., Civerolo, K., Granier, C.,

761 Monks, P. S., Monks, S., Parrish, D. D., Pollack, I. B., Rosenlof, K. H., Ryerson, T. B.,

762 Schneidemesser, E., and Trainer, M.: Analysis of long-term observations of NOx and CO in

763 megacities and application to constraining emissions inventories, Geophys. Res. Lett., 43, 9920-

764 9930, doi:10.1002/2016GL069894, 2016.

765 He, K., Yang, F., Ma, Y., Zhang, Q., Yao, X., Chan, C. K., Cadle, S., Chan, T., and Mulawa, P.: The

766 characteristics of $PM_{2.5}$ in Beijing, China, Atmos. Environ., 35, 4959-4970,

767 https://doi.org/10.1016/S1352-2310(01)00301-6, 2001.

768 He, K. B., Yang, F. M., Duan, F. K., Ma Y. L.: Atmospheric particulate matter and regional complex

769 pollution, Science Press, Beijing, China. 310-327, 2011.

770 Henry, R., Norris, G. A., Vedantham, R., and Turner, J. R.: Source region identification using

771 Kernel smoothing, Environ. Sci. Technol., 43 (11), 4090-4097, http://dx.doi.org/10.1021/

772 es8011723, 2009.

773 Hu, G., Sun, J., Zhang, Y., Shen, X., and Yang, Y.: Chemical composition of $PM_{2.5}$ based on two-

774 year measurements at an urban site in Beijing. Aerosol Air Qual. Res, 15, 1748-1759, 2015.

775 Huang, R. J., Zhang, Y. L., Bozzetti, C., Ho, K. F., Cao, J. J., Han, Y. M., Dällenbach, K. R., Slowik,

776 J. G., Platt, S. M., Canonaco, F., Zotter, P., Wolf, R., Pieber, S. M., Bruns, E. A., Crippa, M., Ciarelli,

777 G., Piazzalunga, A., Schwikowski, M., Abbaszade, G., Schnelle-Kreis, J., Zimmermann, R., An, Z.

778 S., Szidat, S., Baltensperger, U., EI Haddad, I., and Prévôt, A. S. H.: High secondary aerosol

779 contribution to particulate pollution during haze events in China, Nature, 514, 218-222, 2014.

780 Jeong, B., Bae, M. S., Ahn, J., and Lee, J.: A study of carbonaceous aerosols measurement in

781   metropolitan area performed during Korus-AQ 2016 campaign, J. Kor. Soc. Atmos. Environ., 33,

782   2017.

783   Ji, D., Li, L., Wang, Y., Zhang, J., Cheng, M., Sun, Y., Liu, Z. R., Wang, L. L., Tang, G. Q., Hu, B.,

784   Chao, N., Wen, T. X., and Miao, H. Y.: The heaviest particulate air-pollution episodes occurred in

785   northern China in January, 2013: Insights gained from observation, Atmos. Environ., 92, 546-556,

786   2014.

787   Ji, D. S., Wang, Y. S., Wang, L. L., Chen, L. F., Hu, B., Tang, G. Q., Xin, J. Y., Song, T., Wen, T. X.,

788   Sun, Y., Pan, Y. P., and Liu, Z. R.: Analysis of heavy pollution episodes in selected cities of northern

789   China, Atmos. Environ., 50, 338-348, 2012.

790   Ji, D. S., Zhang, J. K., He, J., Wang, X. J., Pang, B., Liu, Z. R., Wang, L. L., and Wang, Y. S.:

791   Characteristics of atmospheric organic and elemental carbon aerosols in urban Beijing, China,

792   Atmos. Environ., 125, 293-306, 2016.

793   Ji, D. S., Yan, Y. C., Wang, Z. S., He, J., Liu, B., Sun, Y., Gao, M., Li, Y., Cao, W., Cui, Y., Hu, B.,

794   Xin, J. Y., Wang, L. L., Liu, Z. R., Tang, G. Q., and Wang, Y. S.: Two-year continuous measurements

795   of carbonaceous aerosols in urban Beijing, China: Temporal variations, characteristics and source

796   analyses, Chemosphere, 200, 191-200, 2018.

797   Ji, D. S., Gao, M., Maenhaut, W., He, J., Wu, C., Cheng, L. J., Gao, W. K., Sun, Y., Sun, J. R., Xin,

798   J. Y., Wang, L. L., and Wang, Y. S.: The carbonaceous aerosol levels still remain a challenge in the

799   Beijing-Tianjin-Hebei region of China: Insights from continuous high temporal resolution

800   measurements in multiple cities, Environ. Int., 126: 171-183, 2019.

801   Jin, Y., Andersson, H., and Zhang, S.: Air pollution control policies in China: a petrospective and

802   prospects, Int. J. Env. Res. Pub. He., 13(12), 1219, 2016.

803   Lang, J., Zhang, Y., Zhou, Y., Cheng, S., Chen, D., Guo, X., Chen, S., Li, X. X., Xing, X. F., and

804   Wang, H. Y.: Trends of $PM_{2.5}$ and chemical composition in Beijing, 2000-2015, Aerosol Air Qual.

805   Res., 17, 412-425, 2017.

806   Li, B., Zhang, J., Zhao, Y., Yuan, S., Zhao, Q., Shen, G., and Wu, H.: Seasonal variation of urban

807   carbonaceous aerosols in a typical city Nanjing in Yangtze River Delta, China, Atmos. Environ.,

808   106, 223-231, 2015.

809   Li, C., Chen, P., Kang, S., Yan, F., Hu, Z., Qu, B., and Sillanpää, M.: Concentrations and light

810 absorption characteristics of carbonaceous aerosol in $PM_{2.5}$ and PM_{10} of Lhasa city, the Tibetan

811 Plateau, Atmos. Environ., 127, 340-346, https://doi.org/10.1016/j.atmosenv.2015.12.059, 2016.

812 Li, C., McLinden, C., Fioletov, V., Krotkov, N., Carn, S., Joiner, J., Streets, D., He, H., Ren, X., Li,

813 Z., and Dickerson, R.: India is overtaking China as the world's largest emitter of anthropogenic

814 sulfur dioxide, Scientific Reports, DOI:10.1038/s41598-017-14639-8, 2017.

815 Li, Y. C., Shu, M., Ho, S. S. H., Yu, J. Z., Yuan, Z. B., Liu, Z. F., Wang, X. X., and Zhao, X, Q.:

816 Effects of chemical composition of $PM_{2.5}$ on visibility in a semi-rural city of Sichuan Basin, Aerosol

817 and Air Qual. Res., 18(4): 957-968, 2018.

818 Liang, Q., Jaeglé, L., Jaffe, D. A., Weiss-Penzias, P., Heckman, A., and Snow, J. A.: Long-range

819 transport of Asian pollution to the northeast Pacific: Seasonal variations and transport pathways of

820 carbon monoxide, J. Geophys. Res-Atmos., 109, doi:10.1029/2003JD004402, 2004.

821 Liu, D., Li, J., Zhang, Y., Xu, Y., Liu, X., Ding, P., Shen, C., Chen, Y., Tian, C., and Zhang, G.: The

822 use of levoglucosan and radiocarbon for source apportionment of $PM_{2.5}$ carbonaceous aerosols at a

823 background site in east China, Environ. Sci. Technol., 47, 10454, 2013.

824 Liu, F., Zhang, Q., Tong, D., Zheng, B., Li, M., Huo, H., and He, K. B.: High-resolution inventory

825 of technologies, activities, and emissions of coal-fired power plants in China from 1990 to 2010,

826 Atmos. Chem. Phys., 15, 13299-13317, https://doi.org/10.5194/acp-15-13299-2015, 2015.

827 Liu, G., Li, J., Wu, D., and Xu, H.: Chemical composition and source apportionment of the ambient

828 $PM_{2.5}$ in Hangzhou, China, Particuology, 18, 135-143, 2015.

829 Lupu A. and Maenhaut, W.: Application and comparison of two statistical trajectory techniques for

830 identification of source regions of atmospheric aerosol species, Atmos. Environ., 36, 5607-5618,

831 2002.

832 Lv, B., Zhang, B., and Bai, Y.: A systematic analysis of $PM_{2.5}$ in Beijing and its sources from 2000

833 to 2012. Atmos. Environ., 124, 98-108, 2016.

834 Malm, W. C., Sisler, J. F., Huffman, D., Eldred, R. A., and Cahill, T. A.: Spatial and seasonal trends

835 in particle concentration and optical extinction in the United States, J. Geophys. Res-Atmos., 99,

836 1347-1370, doi:10.1029/93JD02916, 1994.

837 Miyakawa, T., Kanaya, Y., Komazaki, Y., Miyoshi, T., Nara, H., Takami, A., Moteki, N., Koike, M.,

838 and Kondo, Y.: Emission regulations qltered the concentrations, origin, and formation of

839   carbonaceous aerosols in the Tokyo metropolitan area, Aerosol Air Qual. Res., 16, 1603-1614,

840   10.4209/aaqr.2015.11.0624, 2016.

841   Na, K., Sawant, A. A., Song, C., and Cocker, D. R.: Primary and secondary carbonaceous species

842   in the atmosphere of Western Riverside County, California, Atmos. Environ., 38, 1345-1355,

843   https://doi.org/10.1016/j.atmosenv.2003.11.023, 2004.

844   Niu, X. Y., Cao, J. J., Shen, Z. X., Ho, S. S. H., Tie, X. X., Zhao, S. Y., Xue, H. M., Zhang, T., and

845   Huang, R. J.: $PM_{2.5}$ from the Guanzhong Plain: Chemical composition and implications for emission

846   reductions, Atmos. Environ., 147, 458-469, 2016.

847   Paraskevopoulou, D., Liakakou, E., Gerasopoulos, E., Theodosi, C., and Mihalopoulos, N.: Long-

848   term characterization of organic and elemental carbon in the $PM_{2.5}$ fraction: the case of Athens,

849   Greece, Atmos. Chem. Phys., 14(23), 13313-13325, 2014.

850   Park, J. S., Song, I. H., Park, S. M., Shin, H., and Hong, Y.: The characteristics and seasonal

851   variations of OC and EC for $PM_{2.5}$ in Seoul metropolitan area in 2014, J. Environ. Impact Assess.,

852   24, 578-592, 2015.

853   Peltier, R. E., Weber, R. J., and Sullivan, A. P.: Investigating a liquid-based method for online

854   organic carbon detection in atmospheric particles, Aerosol Sci. Tech., 41, 1117-1127,

855   10.1080/02786820701777465, 2007.

856   Pereira, G. M., Teinilä, K., Custódio, D., Santos, A. G., Xian, H., Hillamo, R., Alves, C. A., Andrade,

857   J. B., Rocha, G. O., Kumar, P., Balasubramanian, R., Andrade M. F., and Vasconcellos, P. C.:

858   Airborne particles in the Brazilian city of São Paulo: One-year investigation for the chemical

859   composition and source apportionment, Atmos. Chem. Phys., 17, 11943-11969, 2017.

860   Petit, J. E., Favez, O., Albinet, A., and Canonaco, F.: A user-friendly tool for comprehensive

861   evaluation of the geographical origins of atmospheric pollution: Wind and trajectory analyses.

862   Environ. Modell. Softw., 88, 183-187, 2017.

863   Poirot, R. L. and Wishinski, P. R.: Visibility, sulfate and air mass history associated with the

864   summertime aerosol in northern Vermont, Atmos. Environ., 20, 1457-1469, 1986.

865   Polissar, A. V., Hopke, P. K., and Harris, J. M.: Source regions for atmospheric aerosol measured at

866   Barrow, Alaska, Environ. Sci. Technol., 35, 4214-4226, 2001.

867   Ram, K. and Sarin, M. M.: Spatio-temporal variability in atmospheric abundances of EC, OC and

WSOC over Northern India, J. Aerosol Sci., 41, 88-98, https://doi.org/10.1016/j.jaerosci.2009.11.004, 2010.

Ram, K. and Sarin, M.: Carbonaceous aerosols over Northern India: sources and spatio-temporal variability, Proc. Indian Natn. Sci. Acad., 78, 523-533, 2012.

Ren, Z. H., Wan, B. T., Yu, T., Su, F. Q., Zhang, Z. G., Gao, Yang, X. X., Hu, H. L., Wu, Y. H., Hu, F., and Hong, Z. X.: Influence of weather system of different scales on pollution boundary layer and the transport in horizontal current field, Res. Environ. Sci., 17(1), 7-13, 2004.

Rollins, A. W., Browne, E. C., Min, K. E., Pusede, S. E., Wooldridge, P. J., Gentner, D. R., Goldstein, A. H., Liu, S., Day, D. A., Russell, L. M., and Cohen, R. C.: Evidence for NOx control over nighttime SOA formation, Science 337(6099), 1210-1212, 2012.

Schauer, J. J., Kleeman, M. J., Cass, G. R., and Simoneit, B. R.: Measurement of emissions from air pollution sources. 5. C1-C32 organic compounds from gasoline-powered motor vehicles, Environ. Sci. Technol., 36, 1169–1180, 2002.

Seinfeld, J. H. and Pandis, S. N.: Atmospheric chemistry and physics: from air pollution to climate change, John Wiley & Sons, 1998.

Shah, J. J., Johnson, R. L., Heyerdahl, E. K., and Huntzicker, J. J.: Carbonaceous aerosol at urban and rural sites in the United States, J. Air Pollut. Control Assoc., 36, 254-257, 1986.

Sharma, S. K. and Mandal, T. K.: Chemical composition of fine mode particulate matter ($PM_{2.5}$) in an urban area of Delhi, India and its source apportionment, Urban Clim., 21, 106-122, https://doi.org/10.1016/j.uclim.2017.05.009, 2017.

Shi, G. L., Peng, X., Liu, J. Y., Tian, Y. Z., Song, D. L., Yu, H. F., Feng, Y. C., and Russell, A. G.: Quantification of long-term primary and secondary source contributions to carbonaceous aerosols, Environ. Pollut. 219, 897-905, 2016.

Sofowote, U. M., Rastogi, A. K., Debosz, J., and Hopke, P. K.: Advanced receptor modeling of near–real–time, ambient $PM_{2.5}$ and its associated components collected at an urban–industrial site in Toronto, Ontario, Atmos. Pollut. Res., 5, 13-23, https://doi.org/10.5094/APR.2014.003, 2014.

Song, Y., Xie, S., Zhang, Y., Zeng, L., Salmon, L. G., and Zheng, M.: Source apportionment of $PM_{2.5}$ in Beijing using principal component analysis/absolute principal component scores and UNMIX, Sci. Total Environ., 372, 278-286, 2006.

897   Tang, G., Zhang, J., Zhu, X., Song, T., Münkel, C., Hu, B., Schäfer, K., Liu, Z., Zhang, J., Wang,

898   L., Xin, J., Suppan, P., and Wang, Y.: Mixing layer height and its implications for air pollution over

899   Beijing, China, Atmos. Chem. Phys., 16, 2459-2475, https://doi.org/10.5194/acp-16-2459-2016,

900   2016.

901   Tao, J., Cheng, T., Zhang, R., Cao, J., Zhu, L., Wang, Q., Luo, L., and Zhang, L.: Chemical

902   composition of $PM_{2.5}$ at an urban site of Chengdu in southwestern China, Adv. Atmos. Sci., 30,

903   1070-1084, 2013.

904   Tao, J., Gao, J., Zhang, L., Zhang, R., Che, H., Zhang, Z., Lin, Z., Jing, J., Cao, J., and Hsu, S. C.:

905     $PM_{2.5}$ pollution in a megacity of southwest China: source apportionment and implication, Atmos.

906   Chem. Phys., 14, 2014.

907   Tao, J., Zhang, L., Cao, J., and Zhang, R.: A review of current knowledge concerning $PM_{2.5}$

908   chemical composition, aerosol optical properties and their relationships across China, Atmos. Chem.

909   Phys., 17(15), 9485-9518, 2017.

910   Villalobos, A. M., Amonov, M. O., Shafer, M. M., Devi, J. J., Gupta, T., Tripathi, S. N., Rana, K. S.,

911   McKenzie, M., Bergin, M. H., and Schauer, J. J.: Source apportionment of carbonaceous fine

912   particulate matter ($PM_{2.5}$) in two contrasting cities across the Indo–Gangetic Plain, Atmos. Pollut.

913   Res., 6, 398-405, https://doi.org/10.5094/APR.2015.044, 2015.

914   Wang, C., An, X., Zhang, P., Sun, Z., Cui, M., and Ma, L.: Comparing the impact of strong and

915   weak East Asian winter monsoon on $PM_{2.5}$ concentration in Beijing, Atmos. Res., 215, 165-177,

916   2019.

917   Wang, J., Allen, D. J., Pickering, K. E., Li, Z., and He, H.: Impact of aerosol direct effect on East

918   Asian air quality during the EAST‐AIRE campaign, J. Geophys. Res-Atmos., 121(11), 6534-6554,

919   2016b.

920   Wang, L., Zhou, X., Ma, Y., Cao, Z., Wu, R., and Wang, W.: Carbonaceous aerosols over China-

921   review of observations, emissions, and climate forcing, Environ. Sci. Pollut. Res., 23(2), 1671-1680,

922   2016a.

923   Wang, P., Cao, J. J., Shen, Z. X., Han, Y. M., Lee, S. C., Huang, Y., Zhu, C. S., Wang, Q. Y., Xu, H.

924   M., and Huang, R. J.: Spatial and seasonal variations of $PM_{2.5}$ mass and species during 2010 in Xi'an,

925   China, Sci. Total Environ., 508, 477-487, https://doi.org/10.1016/j.scitotenv.2014.11.007, 2015.

926   Wang, Y., Khalizov, A., Levy, M., and Zhang, R. Y.: New Directions: light absorbing aerosols and

927   their atmospheric impacts, Atmos. Environ., 81, 713–715, 2013.

928   Wang, Y. Q., Zhang, X. Y., and Draxler, R. R.: TrajStat: GIS-based software that uses various

929   trajectory statistical analysis methods to identify potential sources from long-term air pollution

930   measurement data, Environ. Modell. Softw., 24(8), 938-939, 2009.

931   Wang, Z. S., Zhang, D. W., Liu, B. X., Li, Y. T., Chen, T., Sun, F., Yang, D. Y., Liang, Y. P., Chang,

932   M., Liu, Y., and Lin, A. G.: Analysis of chemical characteristics of $PM_{2.5}$ in Beijing over a 1-year

933   period, J. Atmos. Chem., 73(4): 407-425, 2016c.

934   WHO. Health effects of black carbon. http://wedocs.unep.org/handle/20.500.11822/8699, 2012.

935   Wood, E. C., Canagaratna, M. R., Herndon, S. C., Onasch, T. B., Kolb, C. E., Worsnop, D. R., Kroll,

936   J. H., Knighton, W. B., Seila, R., Zavala, M., Molina, L. T., DeCarlo, P. F., Jimenez, J. L.,

937   Weinheimer, A. J., Knapp, D. J., Jobson, B. T., Stutz, J., Kuster, W. C., Williams, E. J.: Investigation

938   of the correlation between odd oxygen and secondary organic aerosol in Mexico City and Houston.

939   Atmos. Chem. Phys. 18(10), 8947-8968, 2010.

940   Wu, C., Wu, D., and Yu, J. Z.: Quantifying black carbon light absorption enhancement with a novel

941   statistical approach, Atmos. Chem. Phys., 18, 289-309, https://doi.org/10.5194/acp-18-289-2018,

942   2018.

943   Wu, D., Liao B. T, Wu M., Chen, H., Wang, Y., Niao, X., Gu, Y., Zhang, X., Zhao, X. J., Quan, J.

944   N., Liu, W. D., Meng, J., and Sun, D.: The long-term trend of haze and fog days and the surface

945   layer transport conditions under haze weather in North China, Acta Sci Circumst., 34, 1-11, 2014.

946   Wu, H., Zhang, Y. F., Han, S. Q., Wu, J. H., Bi, X. H., Shi, G. L., Wang, J., Yao, Q., Cai, Z. Y., Liu,

947   J. L., and Feng, Y. C.: Vertical characteristics of $PM_{2.5}$ during the heating season in Tianjin, China,

948   Sci. Total Environ., 523, 152-160, https://doi.org/10.1016/j.scitotenv.2015.03.119, 2015.

949   Wu, X., Wu, Y., Zhang, S., Liu, H., Fu, L., and Hao, J.: Assessment of vehicle emission programs

950   in China during 1998–2013: achievement, challenges and implications, Environ. Pollut., 214, 556-

951   567, 2016.

952   Xing, J., Wang, J., Mathur, R., Wang, S., Sarwar, G., Pleim, J., Hogrefe, C., Zhang, Y., Jiang, J.,

953   Wong, D. C., and Hao, J.: Impacts of aerosol direct effects on tropospheric ozone through changes

954   in atmospheric dynamics and photolysis rates, Atmos. Chem. Phys., 17, 9869-9883, 2017.

Xu, J., Wang, Q., Deng, C., McNeill, V. F., Fankhauser, A., Wang, F., Zheng, X., Shen, J., Huang, K., and Zhuang, G.: Insights into the characteristics and sources of primary and secondary organic carbon: High time resolution observation in urban Shanghai, Environ. Pollut., 233, 1177-1187, https://doi.org/10.1016/j.envpol.2017.10.003, 2018.

Yang, F., He, K., Ye, B., Chen, X., Cha, L., Cadle, S.H., Chan, T., and Mulawa, P. A.: One-year record of organic and elemental carbon in fine particles in downtown Beijing and Shanghai, Atmos. Chem. Phys., 5, 1449–1457, 2005.

Yang, F., Huang, L., Duan, F., Zhang, W., He, K., Ma, Y., Brook, J. R., Tan, J., Zhao, Q., and Cheng, Y.: Carbonaceous species in $PM_{2.5}$ at a pair of rural/urban sites in Beijing, 2005-2008, Atmos. Chem. Phys., 11, 7893–7903, 2011a.

Yang, F., Tan, J., Zhao, Q., Du, Z., He, K., Ma, Y., Duan, F., and Chen, G.: Characteristics of $PM_{2.5}$ speciation in representative megacities and across China, Atmos. Chem. Phys., 11, 5207-5219, 2011b.

Yi, K., Liu, J. F., Wang, X. J., Ma, J. M., Hu, J. Y., Wan, Y., Xu, J. Y., Yang H. Z., Liu, H. Z., Xiang, S. L., and Tao, S.: A combined Arctic-tropical climate pattern controlling the inter-annual climate variability of wintertime $PM_{2.5}$ over the North China Plain. Environ. Pollut., 245, 607-615, 2019.

Yu, X. Y., Cary, R. A., and Laulainen, N. S.: Primary and secondary organic carbon downwind of Mexico City, Atmos. Chem. Phys., 9(18), 6793-6814, 2009.

Zhang, F., Zhao, J., Chen, J., Xu, Y., and Xu, L.: Pollution characteristics of organic and elemental carbon in $PM_{2.5}$ in Xiamen, China, J. Environ. Sci., 23(8), 1342-1349, 2011.

Zhang, F., Wang, Z. W., Cheng, H. R., Lv, X. P., Gong, W., Wang, X. M., and Zhang, G.: Seasonal variations and chemical characteristics of $PM_{2.5}$ in Wuhan, central China, Sci. Total Environ., 518-519, 97-105, https://doi.org/10.1016/j.scitotenv.2015.02.054, 2015.

Zhang, R., Jing, J., Tao, J., Hsu, S. C., Wang, G., Cao, J., Lee, C. S. L., Zhu, L., Chen, Z., Zhao, Y., and Shen Z.: Chemical characterization and source apportionment of $PM_{2.5}$ in Beijing: seasonal perspective, Atmos. Chem. Phys., 13, 7053–7074, 2013.

Zhang, R. Y., Khalizov, A. F., Pagels, J., Zhang, D., Xue, H., and McMurry, P. H.: Variability in morphology, hygroscopicity, and optical properties of soot aerosols during atmospheric processing,

984   Proc. Natl. Acad. Sci. U.S.A., 105, 10291–10296, 2008.

985   Zhang, Y., Li, C., Krotkov, N. A., Joiner, J., Fioletov, V., and McLinden, C.: Continuation of long-

986   term global SO_2 pollution monitoring from OMI to OMPS, Atmos. Meas. Tech., 10, 1495-1509,

987   https://doi.org/10.5194/amt-10-1495-2017, 2017.

988   Zhang, Y., Zhang, Q., Cheng, Y., Su, H., Li, H., Li, M., Zhang, X., Ding, A., and He, K.:

989   Amplification of light absorption of black carbon associated with air pollution, Atmos. Chem. Phys.,

990   18, 9879-9896, https://doi.org/10.5194/acp-18-9879-2018, 2018.

991   Zhao, M., Huang, Z., Qiao, T., Zhang, Y., Xiu, G., and Yu, J.: Chemical characterization, the

992   transport pathways and potential sources of $PM_{2.5}$ in Shanghai: Seasonal variations, Atmos. Res.,

993   158, 66-78, 2015a.

994   Zhao, M., Qiao, T., Huang, Z., Zhu, M., Xu, W., Xiu, G., Tao, J., and Lee, S.: Comparison of ionic

995   and carbonaceous compositions of $PM_{2.5}$ in 2009 and 2012 in Shanghai, China, Sci. Total Environ.,

996   536, 695-703, 2015b.

997   Zhao, P., Dong, F., and Yang, Y.: Characteristics of carbonaceous aerosol in the region of Beijing,

998   Tianjin, and Hebei, China, Atmos. Environ., 71, 389-398, 2013.

999   Zheng, B., Tong, D., Li, M., Liu, F., Hong, C., Geng, G., Li, H. Y., Li, X., Peng, L. Q., Qi, J., Yan,

1000 L., Zhang, Y. X., Zhao, H. Y., Zheng, Y. X., He, K. B., and Zhang, Q.: Trends in China's

1001 anthropogenic emissions since 2010 as the consequence of clean air actions, Atmos. Chem. Phys.,

1002 18, 14095–14111, 2018.

1003 Zhu, C., Tian, H., Hao, Y., Gao, J., Hao, J., Wang, Y., Hua, S., Wang, K., and Liu, H.: A high-resolution

1004 emission inventory of anthropogenic trace elements in Beijing-Tianjin-Hebei (BTH) region of China,

1005 Atmos. Environ., 191, 452-462, https://doi.org/10.1016/j.atmosenv.2018.08.035, 2018.

1006
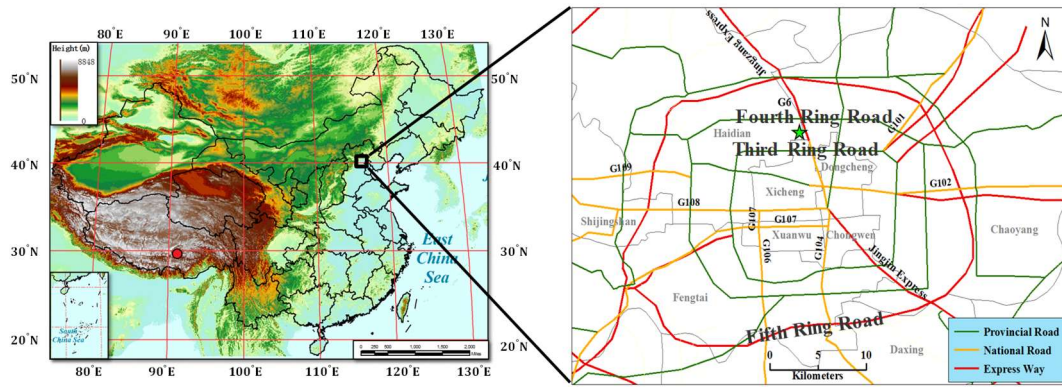
G6=Jingzang Expressway; G101=National Highway 101; G102= National Highway 102; G107= National Highway 107; G108= National Highway 108; G109= National Highway 109

Fig. 1. Map with location of the sampling site (the asterisk in the right figure indicates the sampling site).
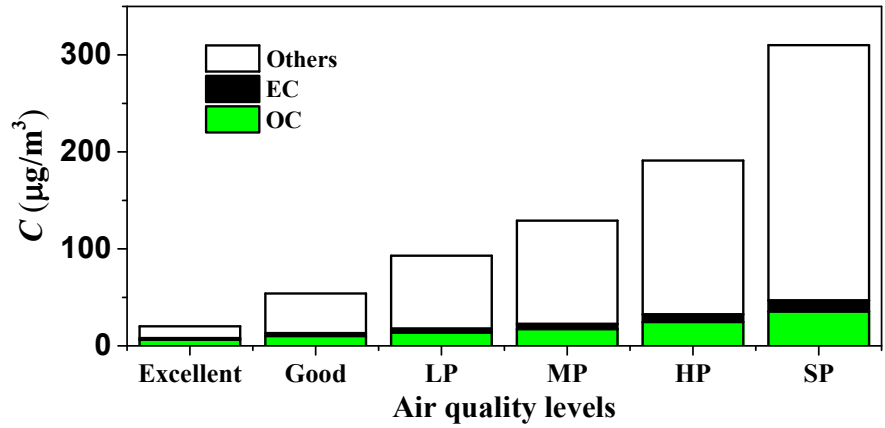
1011
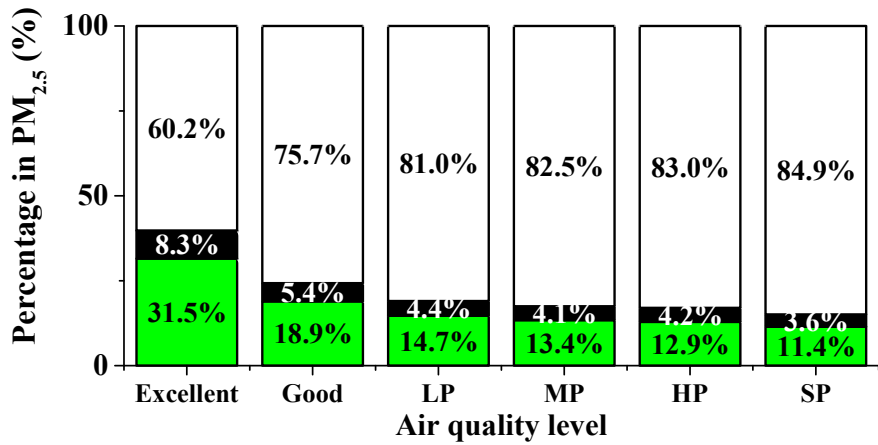
1012

1013 Fig. 2. Variation of average OC, EC and PM$_{2.5}$ concentrations (top) and of the percentages of OC,
1014 EC and other components in PM$_{2.5}$ (bottom) for different air quality levels.

1015
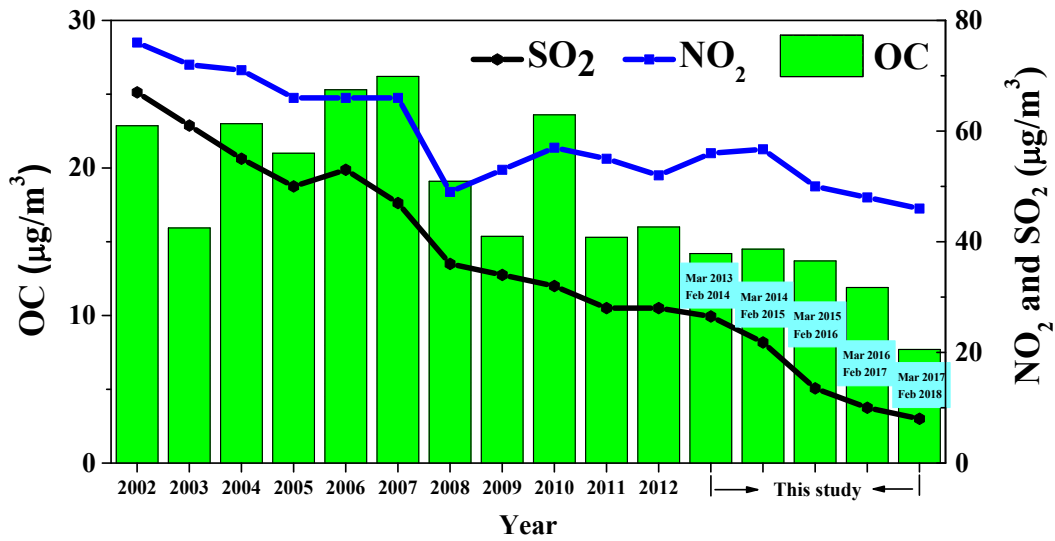
1016
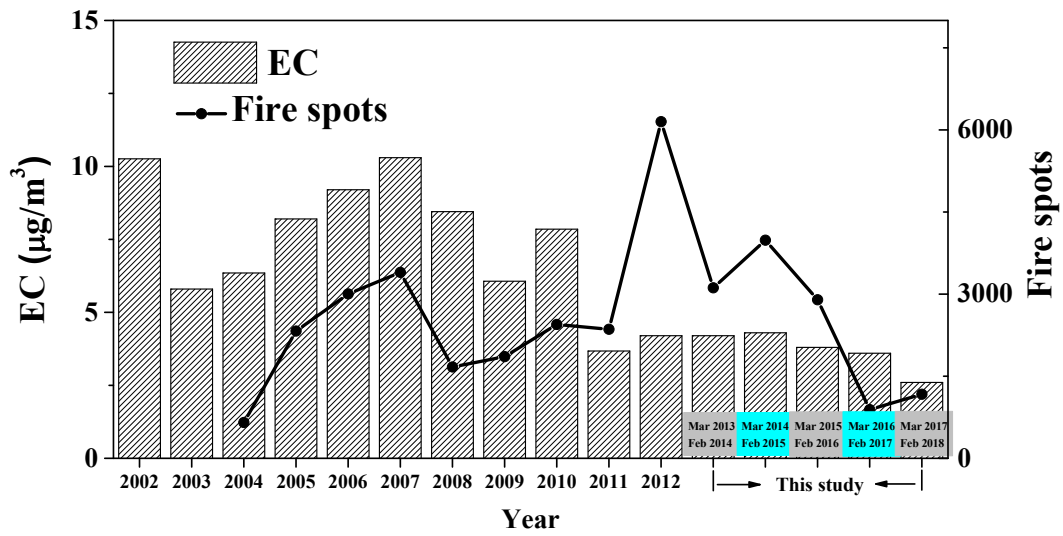
1017

Fig. 3. Variation of the annual mean OC and EC concentrations in PM$_{2.5}$ from 2002 to
2018 in Beijing. The variation in NO$_2$ and SO$_2$ concentrations and in the number of fire
spots counted for the domain of (30-70° N, 65-150° E) is also shown.

1021
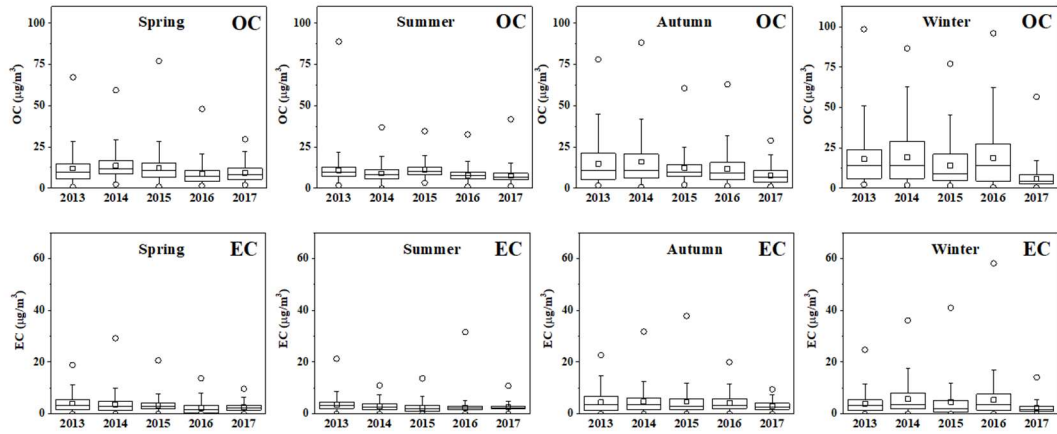
 Fig. 4. Seasonal variations of OC and EC concentrations from March 2013 to February 2018.

1027
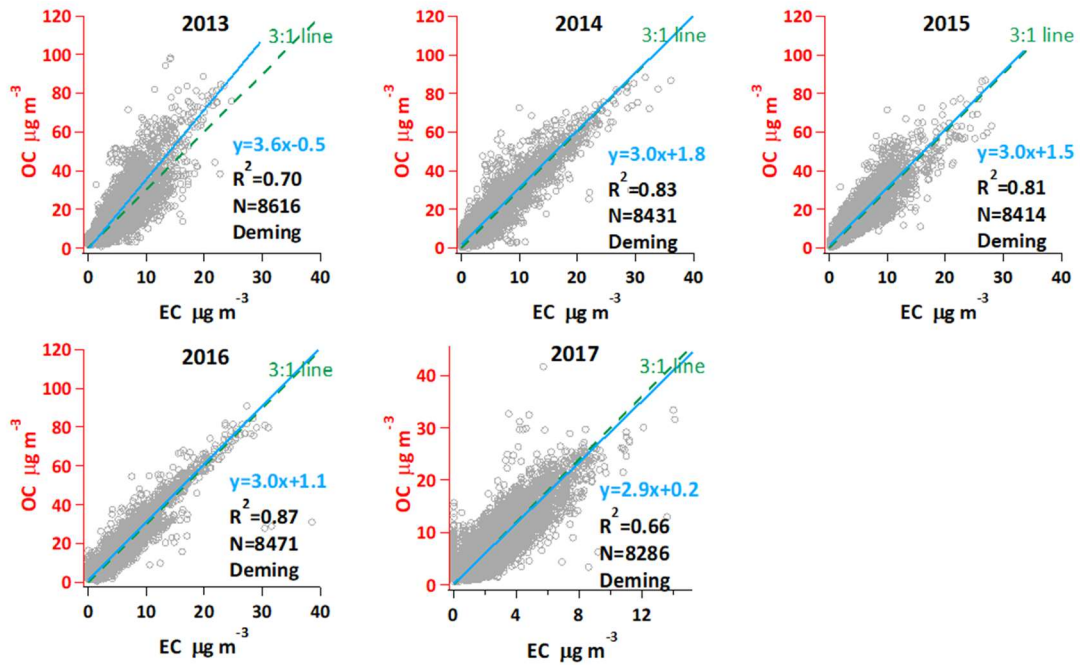
Fig. 5. Relationship between OC and EC using the Deming regression method from 2013 to 2017
(the dashed line indicates a OC/EC ratio of 3:1).

1028

1029

1030
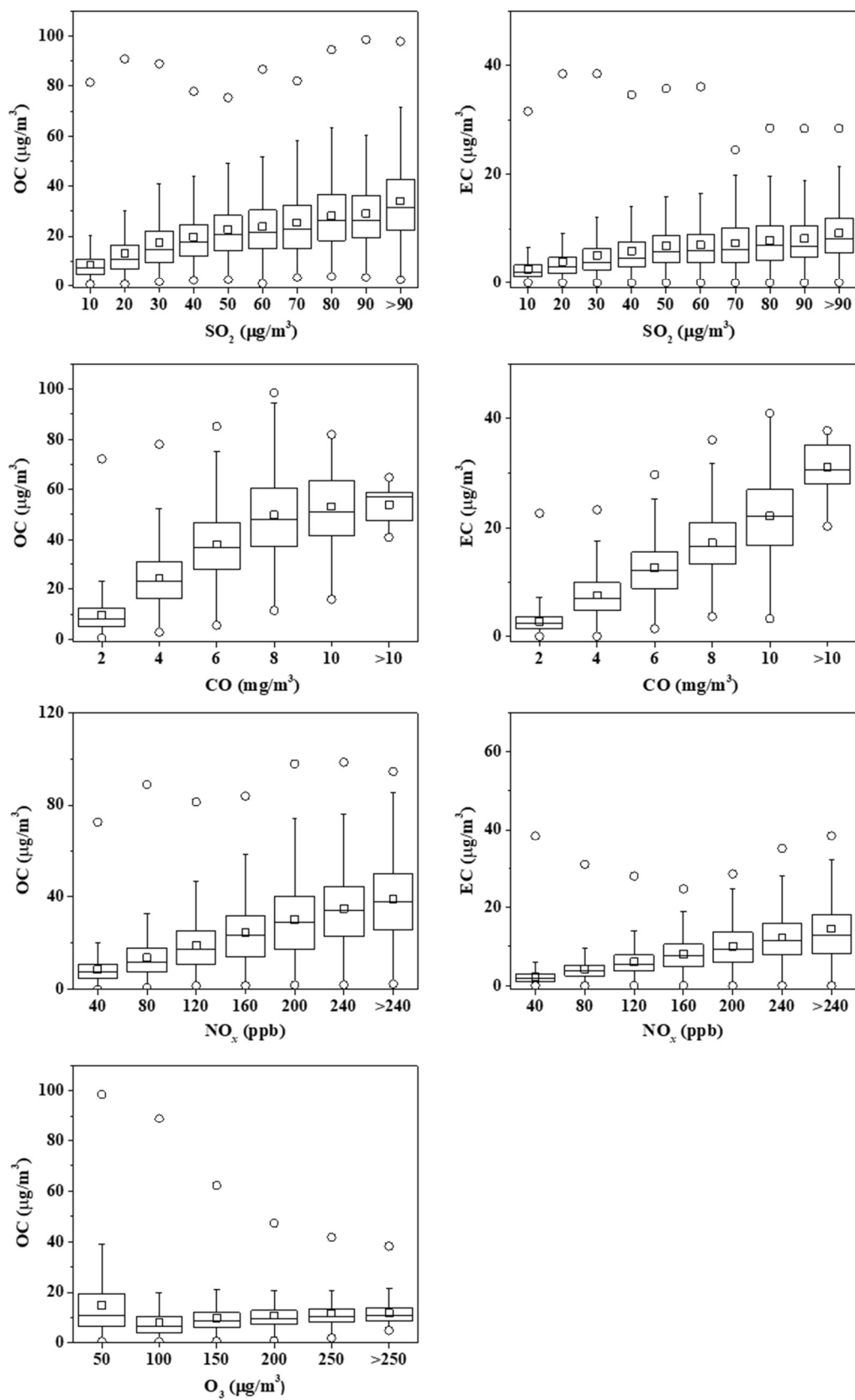
1031

1032   Fig. 6. OC and EC concentrations as a function of the SO_2, CO, NO_x and O_3 concentration.

1033
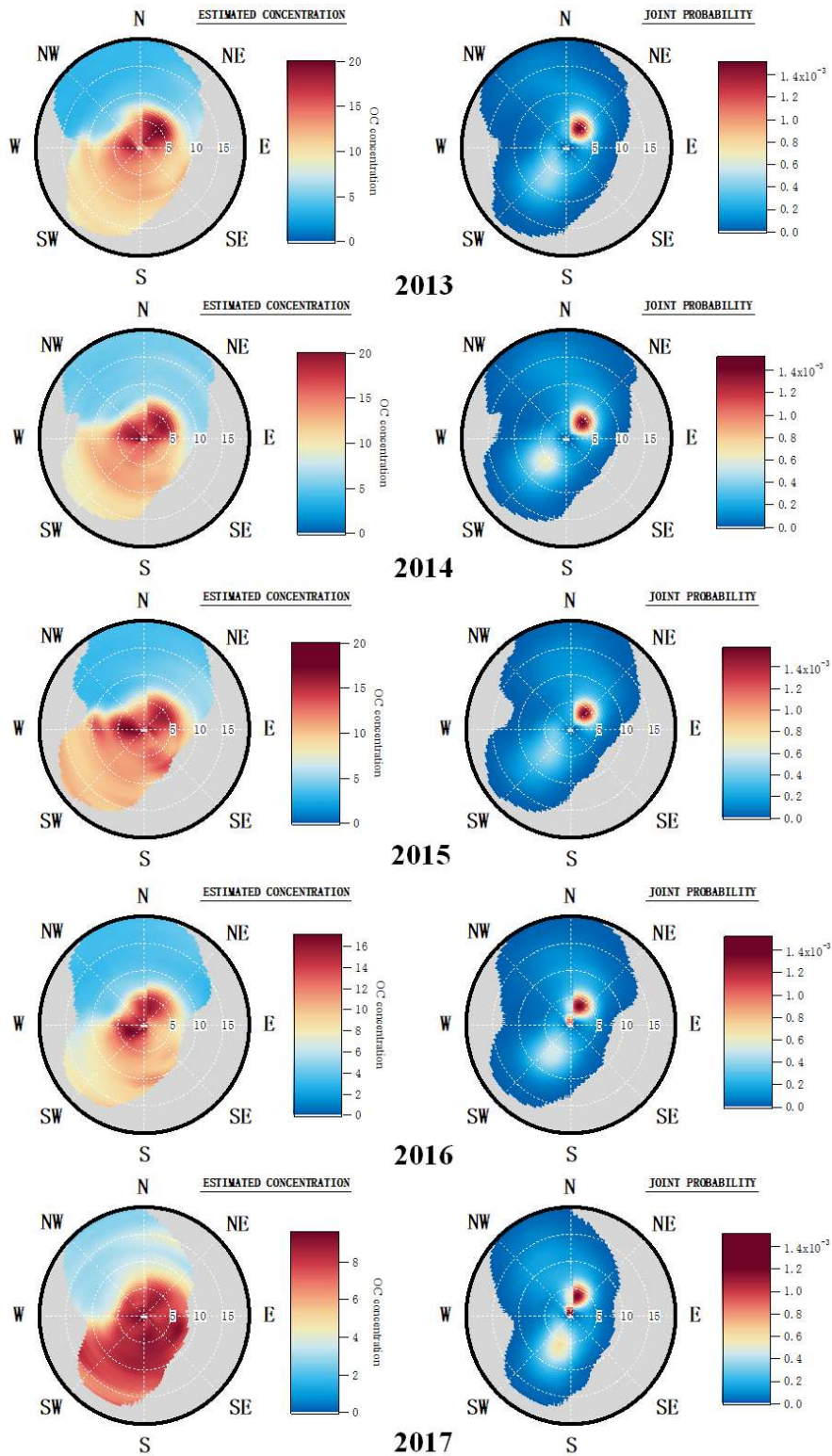
1034

1035 Fig. 7. Wind analysis results using NWR on 1-h OC concentrations measured in Beijing from 2013
1036 to 2017 (Unit of wind speed: km/h).

1037
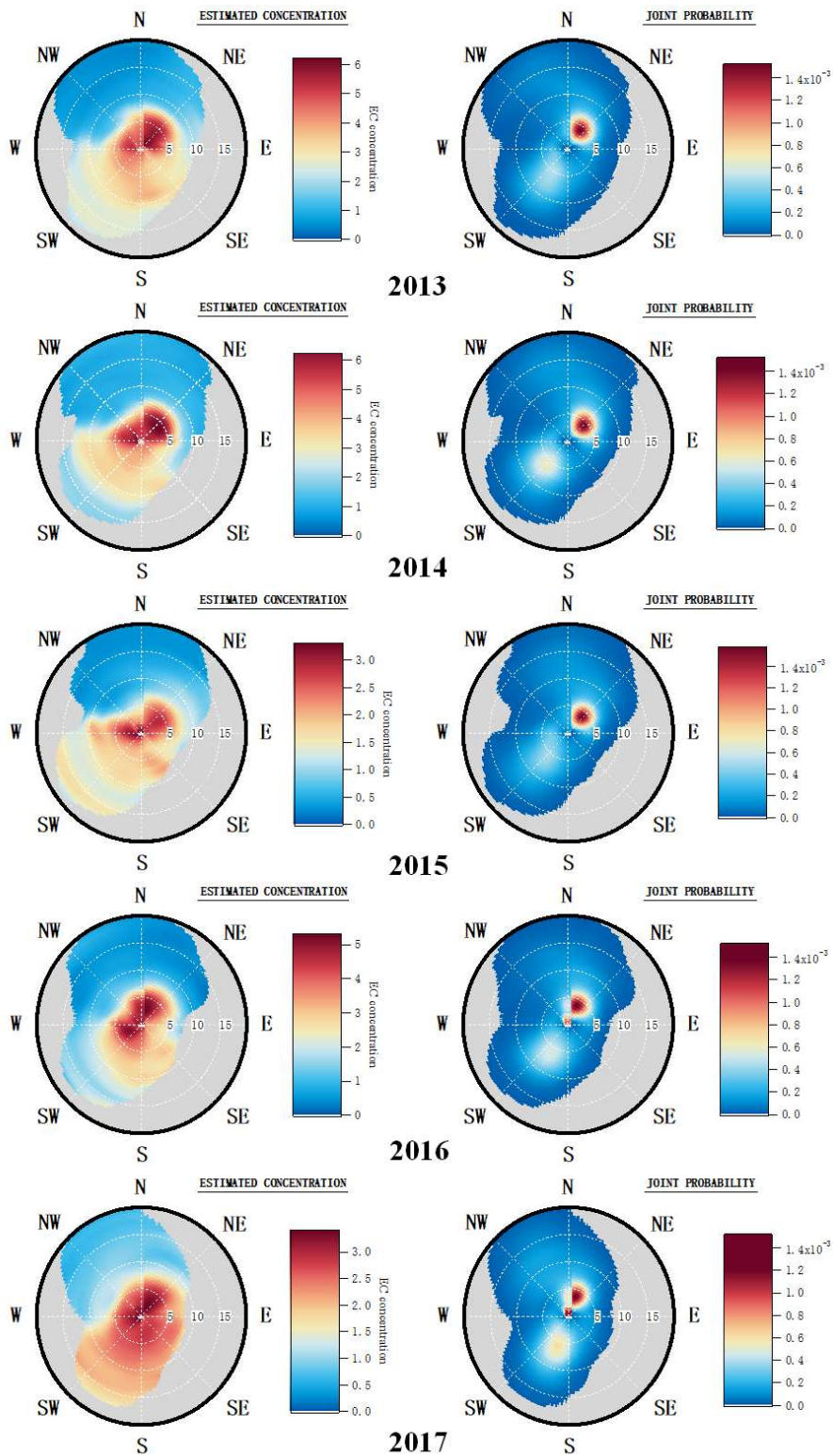
1038

Fig. 8. Wind analysis results using NWR on 1-h EC concentrations measured in Beijing from 2013 to 2017.

1039
1040

1041
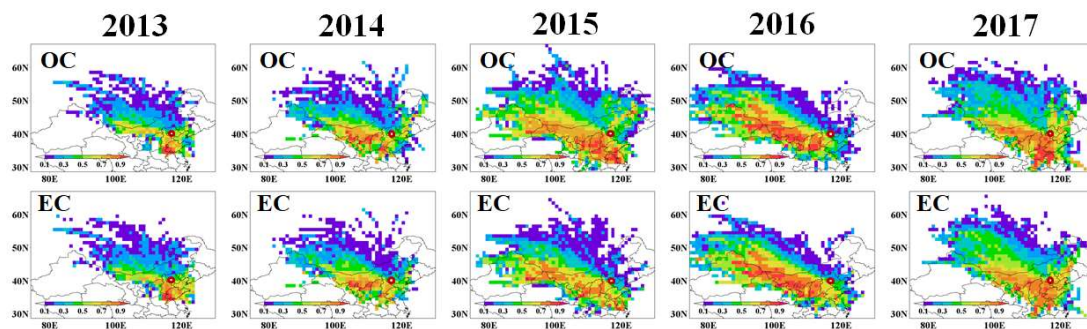
1042

1043 Fig. 9 Potential source areas for OC and EC in Beijing from 2013 to 2017. The color code denotes
1044 the PSCF probability. The measurement site is indicated with a ⬤. The identification of the
1045 provinces is given in Fig. S9.

1046

1047 Table 1. Medians, averages and associated standard deviations for the OC, EC and PM2.5 concentrations (in $\mu g/m^3$) and averages for the OC/PM$_{2.5}$, EC/PM$_{2.5}$ and

1048 TC/PM$_{2.5}$ ratios from March 2013 to February 2018.

	OC			EC			PM$_{2.5}$			OC/PM$_{2.5}$	EC/PM$_{2.5}$	TC/PM$_{2.5}$
	Median	Average	Stdev	Median	Average	Stdev	Median	Average	Stdev	Average	Average	Average
Mar-2013 − Feb-2014	10.6	14	11.7	3.2	4	3.3	66	89	82.9	0.157	0.045	0.203
Mar-2014 − Feb-2015	10.4	14.5	12.1	3	4.3	4	66	85.5	76.6	0.169	0.05	0.219
Mar-2015 − Feb-2016	9.1	13.7	9.2	1.3	3.8	4.4	48	76.9	85.6	0.178	0.049	0.228
Mar-2016 − Feb-2017	8.2	11.9	11.3	2.5	3.6	3.7	53	79.4	82.8	0.15	0.045	0.195
Mar-2017 − Feb-2018	6.8	7.7	4.7	2.3	2.6	1.6	35	49.4	48.6	0.155	0.052	0.208
whole study period	9.3	12.4	10.6	2.7	3.7	3.6	52	75.7	77.6	0.164	0.049	0.213

1049

1050 Table 2. Mean or median OC and EC mass concentrations (in $\mu g/m^3$) observed in major megacities of the world published in the literature and obtained in this study.

1051

1052

Megacities	Method	Period	Number or frequency of sampling	OC	EC	Literature
Athens	TOT	May 2008 to April 2013	Once everyday	2.1	0.54	Paraskevopoulou et al., 2014
Beijing	TOT	March 2017-Feburary 2018	Hourly	7.7	2.6	This study
Hongkong	TOR	from July to October 2014 and December 2014 to March 2015	N=161	7.8	2.2	Chen et al., 2018
Lhasa	TOR	May 2013 to March 2014	once each week	3.27	2.24	Li et al., 2016
Los Angele	TOT	March 2017-Feburary 2018	once every 3 days	2.88	0.56	US EPA*
Mexico	TOT	March 2006	Hourly	5.4-6.4	0.6-2.1	Yu et al., 2009
Mumbai	TOT	March-May 2007, October-November 2007 and December-January 2007-2008	15 days in a season	20.4-31.3	5.0-9.2	Villalobos et al., 2015
New Delhi	TOR	January 2013 -May 2014	N=95	17.7	10.3	Sharma and Mandal, 2017
New York	TOT	March 2017-Feburary 2018	Once every 3 days	2.88	0.63	US EPA*
Paris	TOT	from 11 September 2009 to 10 September 2010	Once everyday	3.0	1.4	Bressi et al., 2013
São Paulo	TOT	2014	Once each Tuesday	10.2	7	Pereira et al., 2017
Shanghai	TOT	from July 2013 to June 2014	Hourly	8.4	3.1	Xu et al., 2018
Soul	TOT	from January 2014 to December 2014	Hourly	4.1	1.6	Park et al., 2015
Tianjin	TOR	from Dec 23, 2013, to Jan 16, 2014	N=25	30.53	8.21	Wu et al., 2015
Tokyo	TOT	from July 27 to August 15, 2014	Once everyday	2.2	0.6	Miyakawa et al., 2016
Toronto	TOT	December 1, 2010-November 30, 2011	Hourly	3.39	0.5	Sofowote et al., 2014
Wuhan	TOT	From August 2012 to July 2013	Once every six days	16.9	2.0	Zhang et al., 2015
Xi'an	TOR	Four months of 2010	N=56	18.6	6.7	Wang et al., 2015

1053 *https://aqs.epa.gov/api

1054 TOR: thermal-optical reflectance; TOT: thermal-optical transmittance

1055 Table 3. OC/EC ratios in main domestic and foreign cities.

	Cities	Period	Method	OC/EC	References
		1999-2000	TOR	2.7	He et al., 2001
		2000	TOT	7.0	Song et al., 2006
		2001-2002	EA	2.6	Duan et al., 2006
		2005-2006	TOT	3.0	Yang et al., 2011b
		2008	TOT	2.2	Yang et al., 2011a
		2008-2010	TOR	4.4	Hu et al., 2015
Domestic cities	Beijing	2009-2010	TOR	2.9	Zhao et al., 2013
		2009-2010	TOT	3.4	Zhang et al., 2013
		2012-2013	TOT	7.0	Wang et al., 2016c
		2013	TOT	5.0	Ji et al., 2018
		2014	TOT	4.8	Ji et al., 2018
		2013	TOT	3.6	This study
		2014	TOT	3.0	This study

	2015	TOT	3.0	This study
	2016	TOT	3.0	This study
	2017	TOT	2.9	This study
Baoji	March 2012 - March 2013	TOR	5.3	Niu et al., 2016
Chengdu	2009-2010 annual	TOR	2.5	Tao et al., 2013
	2009–2013	TOR	4.4	Shi et al., 2016
	2011 annual	TOR	2.4	Tao et al., 2014
	2012-2013 annual	TOT	4.1	Chen et al., 2014
Chongqing	2005-2006 annual	TOR	4.7	Yang et al., 2011b
	2012-2013 annual	TOT	3.8	Chen et al., 2014
	May 2012-May 2013	TOT	3.6	Chen Y. et al., 2017
Ya'an	June 2013 - June 2014	TOT	13.3	Li et al., 2018
Hangzhou	2004-2005 annual	EA	2.0	Liu G. et al., 2015
Hongkong	July - October 2014 and December 2014 - March 2015	TOR	3.5	Chen et al., 2018
Lhasa	May 2013 - March 2014	TOR	1.5	Li et al., 2016

Nanjing	2014 annual	TOT	1.8	Chen D. et al., 2017
	2011-2014 annual	TOR	2.6	Li et al., 2015
Ningbo	2009-2010 annual	TOR	2.8	Liu et al., 2013
Neijiang	2012-2013 annual	TOT	4.5	Chen et al., 2014
Qingling	March 2012 - March 2013	TOR	6.3	Niu et al., 2016
Shanghai	2009 annual	TOR	3.4	Zhao et al., 2015a
	2011	TOT	2.6	Chang et al., 2017
	2012	TOT	2.9	Chang et al., 2017
	2012 annual	TOR	5.4	Zhao et al., 2015b
	2013	TOT	3.4	Chang et al., 2017
Shijiazhuang	Four seasons (2009-2010)	TOR	2.7	Zhao et al., 2013
Tianjin	2009-2010	TOR	2.7	Zhao et al., 2013
Xi'an	2010 annual	TOR	2.7	Wang et al., 2015
	March 2012 - March 2013	TOR	4.0	Niu et al., 2016
	March 2012 - March 2013	TOR	4.0	Niu et al., 2016

		March 2012 - March 2013	TOR	3.8	Niu et al., 2016
		December 2014 - November 2015	TOT	10.4	Dai et al., 2018
	Weinan	March 2012 - March 2013	TOR	4.4	Niu et al., 2016
	Wuhan	From August 2012 - July 2013	TOT	8.5	Zhang et al., 2015
	Athens	May 2008 - April 2013	TOT	3.9	Paraskevopoulou et al. 2014
	Los Angeles	March 2017-Feburary 2018	TOT	5.1	US EPA*
	New Delhi	January 2013 -May 2014	TOR	1.7	Sharma and Mandal, 2017
	New York	March 2017-Feburary 2018	TOT	4.6	US EPA*
Foreign cities	Paris	September 11, 2009 - September 10, 2010	TOT	2.1	Bressi et al., 2013
	São Paulo	2014	TOT	1.5	Pereira et al., 2017
	Seoul	January 2014 - December 2014	TOT	2.6	Park et al., 2015
	Tokyo	July 27 - August 15, 2014	TOT	3.7	Miyakawa et al., 2016
	Toronto	December 1, 2010-November 30, 2011	TOT	6.8	Sofowote et al., 2014

1056   *https://aqs.epa.gov/api

1057   TOR: thermal-optical reflectance; TOT: thermal-optical transmittance; EA: elemental analysis